Structure-Based Design, Synthesis, and Structure−Activity Relationship Studies of Novel Non-nucleoside Adenosine Deaminase Inhibitors

Tadashi Terasaka,*,† Takayoshi Kinoshita,‡ Masako Kuno,§ Nobuo Seki,§ Kohichiro Tanaka,|| and Isao Nakanishi*,‡,#

Medicinal Chemistry Research Laboratories, Basic Research Laboratories, Medicinal Biology Research Laboratories, and Biopharmaceutical and Pharmacokinetic Research Laboratories, Fujisawa Pharmaceutical Co., Ltd., 2-1-6, Kashima, Yodogawa-ku, Osaka 532-8514, Japan

Received December 22, 2003

We disclose herein optimization efforts around the novel, highly potent non-nucleoside adenosine deaminase (ADA) inhibitor, 1-[(*R*)-1-hydroxy-4-(6-(3-(1-methylbenzimidazol-2-yl)propionylamino)indol-1-yl)-2-butyl]imidazole-4-carboxamide **1** (K_i = 7.7 nM), which we recently reported. Structure-based drug design (SBDD) utilizing the crystal structure of the **1**/ADA complex was performed in order to obtain structure−activity relationships (SAR) for this type of compound rationally and effectively. To utilize the newly formed hydrophobic space (F2), replacement of the benzimidazole ring of **1** with a *n*-propyl chain (**4b**) or a simple phenyl ring (**4c**) was tolerated in terms of binding activity, and the length of the methylene-spacer was shown to be optimal at two or three. Replacement of an amide with an ether as a linker was also well tolerated in terms of binding activity and moreover improved the oral absorption (**6a** and **6b**). Finally, transformation of indol-1-yl to indol-3-yl resulted in discovery of a novel highly potent and orally bioavailable ADA inhibitor, 1-[(*R*)-4-(5-(3-(4-chlorophenyl)propoxy)-1-methylindol-3-yl)-1-hydroxy-2-butyl]imidazole-4-carboxamide **8c**.

Introduction

In recent years, adenosine has come to be considered as an important factor in the attenuation of inflammation.[1,2] It has been reported that the concentration of adenosine is increased in inflammatory lesions[3] and that accumulation of adenosine might terminate inflammation. Several reports have indicated that common antirheumatoid drugs, such as methotrexate, aspirin, and sulfasalazine, might exert antiinflammatory action by elevating the extracellular adenosine level.[4] Moreover, the pivotal role of adenosine in the physiological reduction of inflammation was confirmed by using mice deficient in the adenosine A2a receptor. In A2a-deficient mice, subthreshold doses of an inflammatory stimulus that causes minimal inflammation in wild-type mice were sufficient to induce prolonged severe inflammation.[2]

Adenosine deaminase (ADA) (EC 3.5.4.4) is a key enzyme in purine metabolism and catalyzes the irreversible deamination of both adenosine and 2′-deoxyadenosine to inosine and 2′-deoxyinosine, respectively.[5] ADA is ubiquitous in almost all human tissues, and genetic ADA deficiency results in severe combined immunodeficiency disease by impairment of the differentiation and maturation of lymphoid cells.[6] In the past decade, ADA, which was considered to be cytosolic, has also been found on the cell surface via binding to CD26.[7] Since CD26 is strongly up-regulated following T-cell activation, it has been demonstrated that ecto-ADA could perpetuate chronic inflammation by degrading extracellular adenosine or 2′-deoxyadenosine which are toxic for lymphocytes.[8] Therefore, an ADA inhibitor has great potential as an antiinflammatory drug that works at inflamed sites selectively.

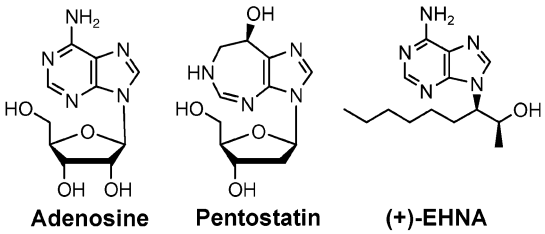

Figure 1. Chemical structures of adenosine and known ADA inhibitors.

Pentostatin (Figure 1) is well-known as a potent transition-state ADA inhibitor.[9] Pentostatin is the only ADA inhibitor in clinical use and is currently approved for the treatment of adult patients with hairy cell leukemia.[10] However, since pentostatin is a nucleoside analogue, it has several toxicities[11] and moreover is not orally bioavailable.[12,13] Therefore, pentostatin cannot be used as an antiinflammatory drug. A number of ground-state ADA inhibitors have been also reported to date besides pentostatin, for example, (+)-EHNA (Figure 1)[14] and related derivatives.[15,16] However, none are used clinically because all are nucleoside analogues or EHNA derivatives and have poor pharmacokinetics, such as rapid metabolism.[17−19] We speculated that the unfavorable properties of the known inhibitors could be im-

* To whom correspondence should be addressed. For T.T.: phone, +81-6-6390-1286; fax, +81-6-6304-5435; e-mail, tadashi_terasaka@po.fujisawa.co.jp. For I.N.: phone, +81-75-753-9273; fax, +81-75-753-9273; e-mail, isayan@pharm.kyoto-u.ac.jp.
† Medicinal Chemistry Research Laboratories.
‡ Basic Research Laboratories.
§ Medicinal Biology Research Laboratories.
|| Biopharmaceutical and Pharmacokinetic Research Laboratories.
Current address: Department of Theoretical Drug Design, Graduate School of Pharmaceutical Sciences, Kyoto University, Sakyo-ku, Kyoto 606-8501, Japan.

10.1021/jm0306374 CCC: $27.50
Published on Web 06/17/2004

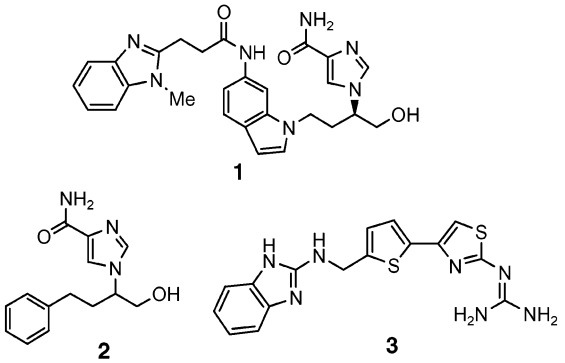

Figure 2. Chemical structures of hybrid compound **1** and the structurally distinct lead compounds **2** and **3**.

proved by changing the nucleoside framework to a non-nucleoside framework and initiated a search for non-nucleoside ADA inhibitors.[19] Despite the difficulty of converting a nucleoside to non-nucleoside, a recent report from our laboratories has described the discovery of a novel, highly potent non-nucleoside ADA inhibitor **1** (K_i = 7.7 nM to human ADA) (Figure 2).[20] This compound was discovered by intentional hybridization of two structurally distinct lead compounds [**2** (K_i = 5.9 μM) and **3** (K_i = 1.2 μM)] by only two structure-based drug design (SBDD) iterations (Figure 2), and as a result, no detailed information on structure−activity relationships (SAR) for the hybrid compound was available. Therefore, we next attempted to optimize compound **1** based on the crystal structure of the **1**/ADA complex in order to obtain SAR and to improve activity and pharmacokinetic properties. In this paper we disclose these optimization efforts and the discovery of several analogues with higher inhibitory potency for ADA.

Results and Discussion

Compound **1** has a novel structure and highly potent ADA inhibitory activity, so we opted to perform further studies based around this structure. The crystal structure of the **1**/ADA complex revealed that ADA performed an induced fit to bind **1**. That is, compound **1** utilized newly formed binding pockets in the enzyme that are spatially distinct from the pockets occupied by substrate-like inhibitors.[20] A narrow planar hydrophobic space (F1) is occupied by the 6-acylaminoindole ring and the comparatively large hydrophobic space (F2) is occupied by the benzimidazole ring (Figure 3a). This information proved very useful for the subsequent design of novel ADA inhibitors because no comparable data for a semi-tight-binding inhibitor such as EHNA is available. As a result, we decided to investigate the SAR for the newly formed binding pockets (F1 and F2). According to the crystal structure of the **1**/ADA complex, the benzimidazole ring binds tightly to the F2 pocket so there is hardly any space to introduce substituents from the 4- to 7-positions except for the space to the outside of the active site(solvent region) (Figure 3a). Hence, we initially decided to modify the benzimidazole part of **1** in order to obtain SAR for this part of the structure and discover structures more amenable to rapid synthetic modification, while retaining highly potent ADA inhibitory activity.

1. Amide-Linked Compounds. Removal of the benzimidazole moiety from **1** to give the acetyl analogue **4a** resulted in a substantial deterioration (170-fold) in the inhibitory potency due to elimination of the van der Waals and/or hydrophobic interactions with the F2 space (Table 1). However, replacement of the benzimidazole ring of **1** with a *n*-propyl chain (**4b**) or a simple phenyl ring (**4c**) was a tolerated modification in terms of binding activity. These modifications resulted in about a 3-fold loss in ADA inhibitory potency (K_i = 24 and 30 nM, respectively) (Table 1), which strongly suggests that extension of the molecule from the indolyl ring of **4a** to the F2 space is important for high potency due to energy gains from more favorable van der Waals or hydrophobic interactions. Although compounds **4b** and **4c** have similar activity, compound **4c** was chosen for further SAR studies due to synthetic expediency.

Table 1. Inhibition Constants for Amide-Linked Derivatives of **1** with ADA

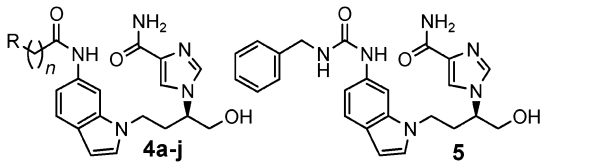

compd	R	*n*	K_i (nM)[a]
1	-	-	7.7[b]
4a	H	1	1300
4b	*n*-C_3H_7	2	24
4c	Ph	2	30
4d	Ph	3	16
4e	Ph	4	11[c]
4f	Ph	5	91
4g	4-Me-Ph	2	38
4h	4-MeO-Ph	2	57
4i	4-Me-Ph	3	34
4j	3-Py	2	17
5	-	-	7.5[c]

[a] K_i values were measured with human ADA. Assays were performed in duplicate. [b] Reference 20. [c] Tight-binding inhibitory mode.

Table 2. Simulated Interaction Energies for Methylene-Inserted Analogues of **4c**

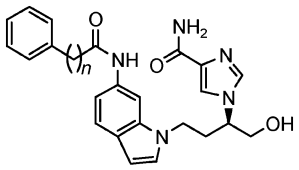

	n = 2	*n* = 3	*n* = 4	*n* = 5	*n* = 6
E (kcal/mol)[a]	−115.2	−115.1	−115.7	−120.9	−110.1

[a] Calculated interaction energies.

Inspection of the docking simulation of **4c** with ADA indicated that the distal hydrophobic space (F2) of the active site, where the phenyl ring resides, is not fully occupied by the inhibitor molecule. Hence, in addition to **4c**, we designed compounds possessing methylene chains of varying lengths between the indole moiety and the phenyl ring, and docking simulation of the designed compounds with ADA based on the **1**/ADA complex was performed to prioritize the synthesis. Table 2 shows the calculated interaction energies of the designed compounds. Since calculated interaction energies consider only nonbonded energy terms, but not desolvation energies and other entropic factors, they do not accurately reflect affinities of ligands. Moreover, since the

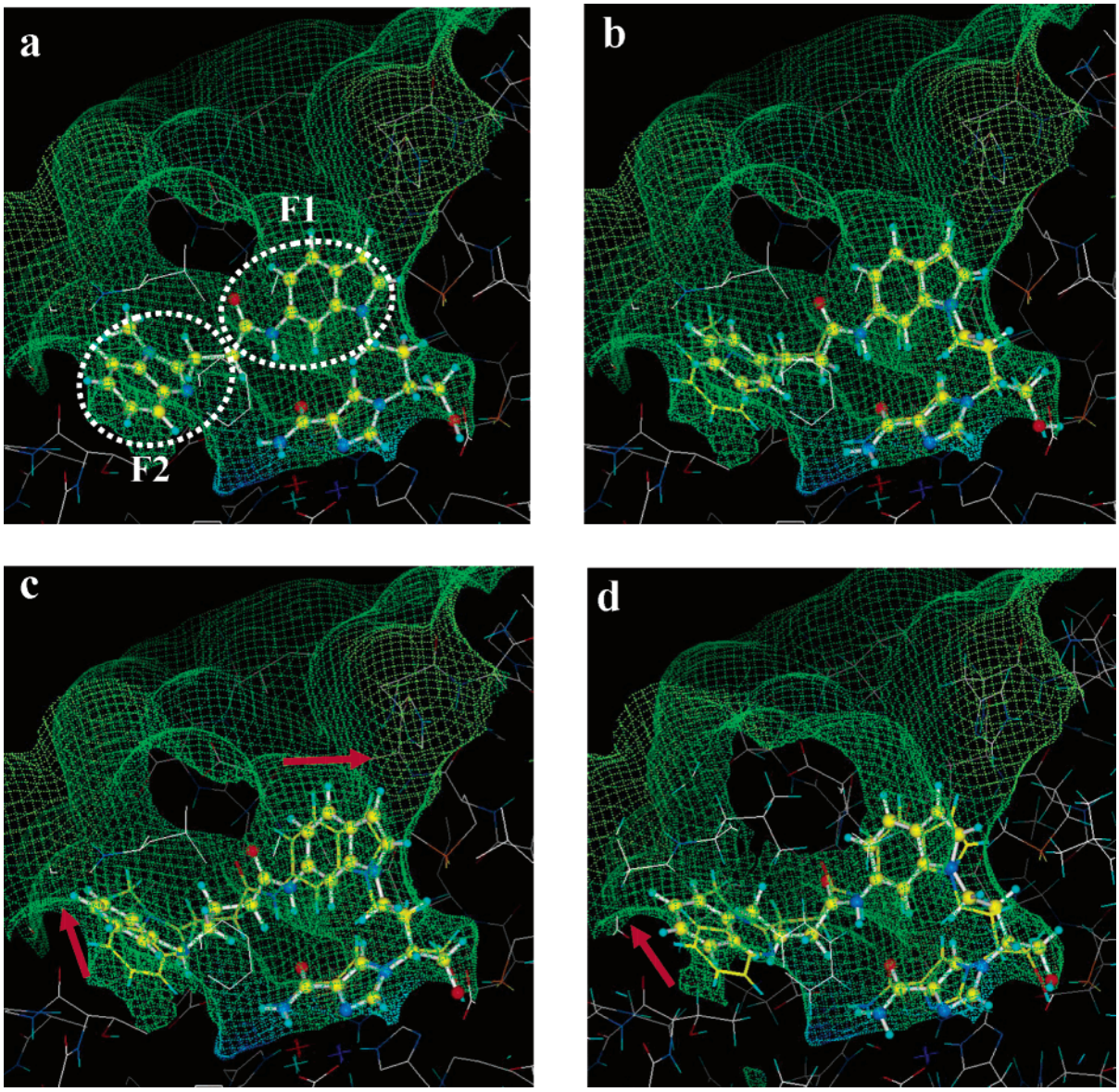

Figure 3. Binding mode of **1** and amide-linked compounds at the ADA active site. Accessible surfaces of the carbon atoms at the active sites are drawn by mesh. Because the active site is located on the inside of protein, meshed regions indicate regions where inhibitor molecules can exist without contact to the proten. The upper portion of the figures is the active site entrance (solvent region). Residues of ADA around the active site are drawn by wire model. Several residues are omitted for clarity. Inhibitor molecules are rendered as ball-and-stick models colored by atom type: yellow for C, blue for N, red for O, and cyan for H. (a) Binding orientations of **1** (PDB code: 1NDZ). (b and c) Binding orientations of **4c** (PDB code: 1UML) and **4e** (PDB code: 1QXL) (ball-and-stick), respectively, with **1** (stick) superimposed onto the active site surface of the **1**/ADA complex. (d) Simulated binding mole of **4d** (ball-and-stick) and **1** (stick) superimposed onto the active site surface of the **4c**/ADA complex. The displacements between **1** and inhibitors are shown with red arrows in c and d.

F2 pocket is a comparatively large hydrophobic space, it was difficult to predict the precise position of the phenyl ring in F2 from molecular modeling. However, we adopted interaction energy to evaluate unfavorable intermolecular interactions such as large interatomic clashes or electrostatic repulsions. From this point of view, methylene chains from three to five carbons in length could be readily accommodated by the binding site, because their E values are similar or lower than that of the two-carbon chain compound (**4c**). However, the compound with six methylenes is unsuitable for binding to the F2 space, because the E value is higher ($\Delta E > 5$ kcal/mol) than the others. Therefore, compounds **4d**−**f** were synthesized and evaluated (Table 1). Consequently, compounds **4d** and **4e** exhibited more potent inhibitory activities compared to **4c**; however, the five methylene chain compound (**4f**) led to a 3-fold decrease in enzyme inhibitory potency. Before the docking simulations were performed, we had considered from the crystal structure of the **1**/ADA complex that four (**4e**) and five (**4f**) methylene chains were too long to fit the phenyl ring to the F2 space in a similar manner as the benzimidazole ring of **1**, but molecular modeling predicted that they could fit to the binding site as described above although these phenyl rings located almost outside of the F2 pocket. To clarify the binding mode of **4c** and **4e** and obtain information for the next design stage, we carried out determination of the crystal structures of complexes with ADA. The crystal structure of the **4c**/ADA complex revealed that more space is available for binding with ADA in the distal F2 space and the other portions of **4c** showed the same binding

mode as **1** (Figure 3b). On the other hand, the crystal structure of the **4e**/ADA complex revealed that the indolyl ring had shifted to close proximity to the wall of the active site compared to **1**, and moreover the phenyl ring shifted to the upper position of the F2 pocket, connected to the outside of the active site (solvent region), compared to the benzimidazole ring of **1** (Figure 3c). Accordingly, compound **4e** could fit to the active site without clashes with the enzyme wall and display high inhibitory potency. Compound **4e**, however, shows a different inhibition mode compared to the others (i.e. tight-binding inhibition like pentostatin). When pentostatin was analyzed by testing different concentrations with different enzyme concentration, the plot of enzyme velocity against enzyme concentration (Ackermann−Potter plot) was characterized by asymptotic concave curves, which revealed the tight-binding or stoichiometric nature of the inhibitor.[21] Compound **4e** produces the same pattern as pentostatin in an Ackermann-Potter plot (data not shown). By inspecting in detail the crystal structure of the **4e**/ADA complex compared to that of **1** or **4c**/ADA, several differences in the binding mode of **4e** were detected; however, we are unsure as to the exact reason for such an observation. The inhibitory mode of pentostatin is suspected to be the reason for chronic inhibition and severe immunodeficiency. Therefore, we did not perform further studies with **4e** but rather with the competitive inhibitors (**4c** and **4d)** to obtain SAR for binding to the distal hydrophobic pocket.

It was considered from the crystal structure of the **4c**/ADA complex (Figure 3b) that more space exists to introduce substituents onto the phenyl ring in F2. On the other hand, the docking simulation of the **4d**/ADA complex (Figure 3d) shows that the phenyl ring of **4d** shifted to the upper position of the F2 pocket compared to the benzimidazole ring of **1**, hence does not utilize the F2 pocket substantially. Moreover, the distal phenyl ring is adjacent to the wall of the active site, in particular, the para position of the phenyl ring, and there is no space to introduce a substituent. Therefore, it was considered that a compound containing a substituent in the para position of the phenyl ring would not bind to the active site. On the other hand, crystal structure analyses of complexes of ADA with our inhibitors (**1**, **4c**, and **4e**) revealed that ADA performed induced fit to bind our inhibitors and that the shape of the F2 pocket is changeable (Figure 3). Furthermore, the para-substituted phenyl analogue of **4d** could fit to the active site of ADA by shifting the indolyl ring and the phenyl ring, as shown by the crystal structure of the **4e**/ADA complex (Figure 3c). Hence, we considered that it was important for subsequent design to investigate the limitations of the F2 pocket and obtain the SAR. From the reasoning described above, we designed and synthesized the substituted phenyl analogues (**4g**, **h**, **i**) of compounds **4c** and **4d**. This resulted in similar or a small deterioration of inhibitory activity (Table 1). Occupying the nonutilized spaces on binding of **4c** (**4g**, **h**) was not effective to enhance the inhibitory potency. That is, a methyl group is tolerated, but a methoxy group is a little too large, although compound **4h** can still bind to the active site. On the other hand, compound **4i** was tolerated in terms of binding activity (2-fold loss relative to **4d**), despite lack of space to introduce substituents in the para position of the phenyl ring of **4d**. This observation suggests that either the active site changes to bind **4i** or the indolyl ring and/or the substituted phenyl ring of **4i** shift to appropriate positions in the active site to fit to ADA.

So far we had replaced the benzimidazole of compound **1** with hydrophobic phenyl or alkyl chains, because it was considered that the F2 space was highly hydrophobic. However, the benzimidazole is a basic heterocyclic ring, so we also attempted to replace the phenyl ring of **4c** with a basic heterocyclic ring, pyridine (**4j**). This replacement resulted in a 2-fold increase in inhibitory activity relative to the phenyl analogue (**4c**) (Table 1). Although F2 is a hydrophobic region, the result for **4j** and the potency of **1** suggests tolerance and a possible preference for occupation of the F2 space by basic heterocyclic rings and provides useful information for further optimization.

From the study described above, we obtained comparative SAR information for utilizing the F2 space, for example, the possibility of simple aromatic rings instead of benzimidazole and the permissible length of spacer compatible with this site. Taking advantage of this information, we next investigated the possibility of transformation of the amide-linker that connected with the indolyl ring.

2. Transformation of the Amide-Linker Connecting the Indole to the F2 Site Binding Moiety. 2-1. Urea-Linked Compounds. In consideration of the narrow planar space available at F1 and conformational restriction of the designed compound, an amide group was introduced at the 6 position of the indolyl ring to extend the molecule to the F2 region. It was considered that this group also plays a role to form an intramolecular hydrogen bond between the NH and the carbonyl of the imidazolecarboxamide. Further, the crystal structures of the **1** and **4c**/ADA complexes verified formation of an intramolecular hydrogen bond (distances between C═O and HN are 3.0 and 3.2 Å, respectively), but they were not tight bonds. It is well-known that restricting the flexibility of a molecule can enhance the potency of an inhibitor.[22] To enhance ADA inhibition potency, we next studied conformational restriction of compound **4c**. In consideration of the formation of a tight intramolecular hydrogen bond with the carbonyl group of the imidazole ring, we replaced the methylene neighboring the carbonyl group of **4c** with NH, which led to urea type compound **5**. This compound was found to be 4-fold more potent than **4c** in the ADA inhibitory assay with a K_i of 7.5 nM. A crystal structure of the **5**/ADA complex verified that compound **5** bound to the active site of ADA in a manner similar to **4c**, but contrary to our expectation, the NHs of the urea moiety of **5** did not form intramolecular hydrogen bonds, as shown in Figure 4. That is, the distances of 3.3 and 3.5 Å between C═O and the two HNs are a little too long for a strong hydrogen bond (typical length = 2.5−3.0 Å). In search of a possible explanation for this observation, we carefully analyzed the nature of the interaction of **4c** and **5** with the active site of ADA (Figure 4b). Both inhibitors formed hydrogen bonds with ADA through the hydroxyl and imidazolecarboxamide moieties to H17, D19, G184, E217, and D296, directly or by bridging through structural waters. However, the carbamoyl group of the

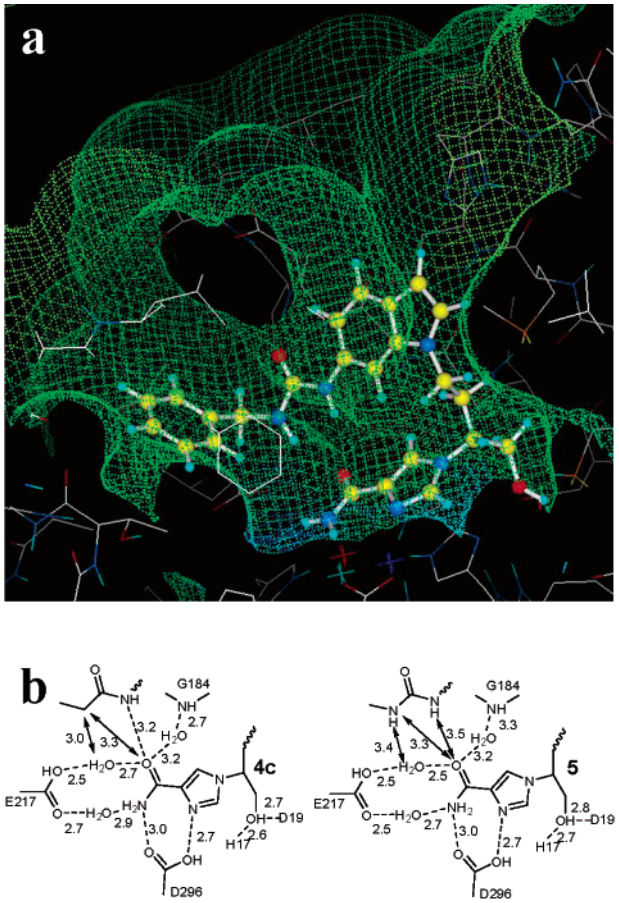

Figure 4. (a) Binding orientations of **5** (ball and stick)/ADA complex (PDB code: 1O5R). (b) Hydrogen bond networks around the carboxamide moieties of **4c** (left) and **5** (right). Hydrogen bonds are drawn by dashed lines with the bonding distance.

imidazole ring of **5** forms more tight hydrogen bonds with ADA through three structural water molecules than that of **4c**. Furthermore, repulsion between the methylene neighboring the carbonyl group of **4c** and a water molecule bridging the carbamoyl group of the imidazole ring to E217 (d = 3.0 Å) was observed, but not for the NH neighboring the carbonyl group of **5** (d = 3.4 Å). This result suggests that the intramolecular hydrogen bond is a favorable, but not essential, factor for highly potent ADA inhibition within this series. Although compound **5** showed high ADA inhibitory potency, it displayed a different inhibitory mode compared to the other analogues, similar to **4e**. The reason for the change in inhibition mode is unclear at present. We did not perform further studies with **5** for the same reason as with **4e**.

2-2. Ether Linked Compounds. From the study described above, we considered that the amide-linker that connected with the indolyl ring is changeable, because the intramolecular hydrogen bond might be not essential for potent ADA inhibition. Moreover, according to the 'rule of five',[23] it was predicted that because the amide- and urea-linked compounds described above have a high sum of hydrogen bonds acceptors (Ha) and donors (Hd), they may have poor oral absorption and permeability (Ha/Hd for compounds **1** and **5** are 10/4 and 9/5, respectively). Hence, we next designed ether-linked compounds **6a** and **6b** based on the amide-linked

Table 3. Inhibition Constants for Ether-Linked Indol-1-yl Derivatives with ADA

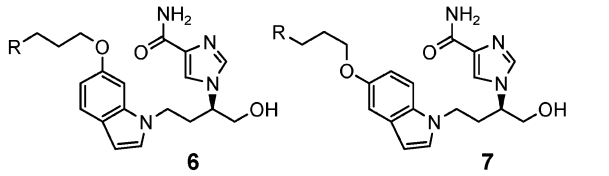

compd	R	K_i (nM)[a]
6a	Ph	17
6b	$PhCH_2$	12
6c	n-C_3H_7	55
6d	Me	240
6e	4-Cl-Ph	13
7a	Ph	1900
7b	n-C_3H_7	6200

[a] See footnote *a* of Table 1.

compounds **4c** and **4d** (Table 3), for which Ha/Hd = 7/3, to reduce the sum of hydrogen bonds and to discover improved compounds in terms of oral absorption.

Ether-linked compounds **6a** and **6b** were found to be more potent in terms of binding activity than the corresponding amide-linked compounds **4c** and **4d**, respectively (Table 3), despite not forming an intramolecular hydrogen bond. These results support our hypothesis. Comparison of the ether-linked compounds **6a** and **6b** with the corresponding amide-linked compounds **4c** and **4d** indicates that the ether-linked compounds can form a hydrogen bond with ADA through the hydroxyl and imidazolecarboxamide moieties in a manner similar to amide-linked compounds, but could not form the intramolecular hydrogen bond. Moreover, dipole repulsion of the oxygen of the ether with the C═O of carbamoyl of imidazole ring is expected. This is a potential disadvantage for ether-linked compounds; however, desolvation energies for the ether-linked compounds are predicted to be lower than for the amide-linked compounds because the number of heteroatoms is reduced. Repulsion between oxygen of the ether and C═O of the carbamoyl is compensated by reduced desolvation energies. In addition to potent activity, compounds **6a** and **6b** showed oral absorption in rats in preliminary studies of oral administration, in contrast to no detectable serum levels with amide-linked compounds **1** and **4d** (data not shown). These results motivated us to further SAR studies in this series. Replacement of the phenyl ring of **6a** with a simple methylene chain, such as *n*-propyl (**6c**) was tolerated in terms of binding activity (3-fold loss), but a methyl (**6d**) led to a 14-fold loss in inhibitory potency (Table 3). These results were similar to the SAR of the amide-linked series. That is, sufficient occupancy of the F2 pocket with these molecules is crucial for highly potent ADA inhibition.

Since the ether-linked compounds are not able to form an intramolecular hydrogen bond like the amide compounds, we considered that it is not necessary to connect at the 6-positon of the indolyl ring. Therefore, in addition to 6-substituted ether-linked compounds, we designed 5-substituted ether-linked types **7a** and **7b** to determine the best link position. Molecular modeling studies of **6a** and **7a** with ADA show that the E value of **7a** is lower (ΔE = ca. 1 kcal/mol) than that of **6a**; however, the indolyl ring of **7a** shifted compared to that

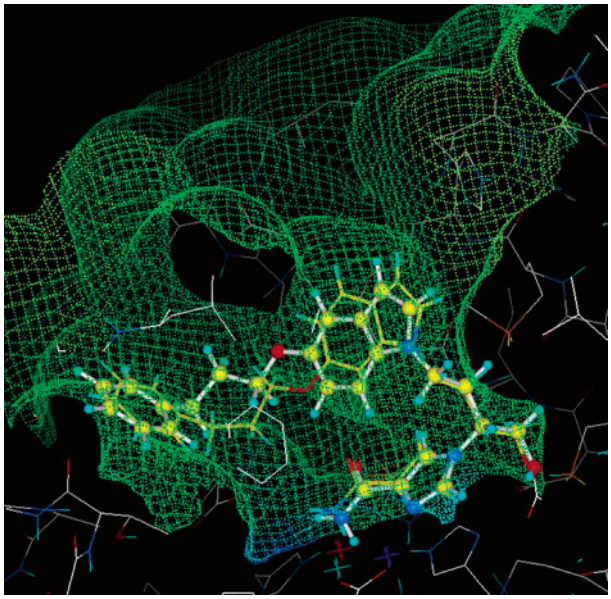

Figure 5. Simulated binding mode of **7a** (ball and stick) and **6a** (stick) superimposed onto the active site surface of the **1**/ADA complex.

of **6a** (Figure 5). It is predicted that the structure of **7a** is strained in order to fit to the active site without clashes with the enzyme wall. Indeed the modeling showed that the internal energy of **7a** is higher (ΔE = ca. 4 kcal/mol) than that of **6a**, so that compound **7a** is less stable than **6a**. That is, 5-substituted ether-linked compound (**7a**) has a lower interaction energy but higher internal (strain) energy than 6-substituted ether-linked compound (**6a**) in order to fit to the active site. Compounds **7a** and **7b** were actually synthesized and evaluated, and consequently these compounds showed a drastic reduction of inhibitory activity (Table 3) as predicted. Hence, further SAR studies on this type were not performed.

Inspection of the binding mode of **6a** indicates that there is more space available for binding with ADA in the F2 region (Figure 5). In the study of amide-linked compounds, however, introducing methyl or methoxy groups at the para position of the phenyl ring was not effective to enhance the inhibitory potency. It was considered that more planar substituents than methyl or methoxy groups may be acceptable for binding to the F2 space. Moreover, an unsubstituted phenyl ring is relatively susceptible to oxidative metabolism, and it is well-known that introduction of a halogen atom at the para position of the phenyl ring can protect from metabolism.[24] Therefore, we designed the *p*-chlorophenyl compound of **6a**. The resulting compound (**6e**) showed high potency compared to **6a** (Table 3). This approach is effective to enhance the inhibitory potency and potentially protect the phenyl ring from metabolism. Hence, we also adopted the *p*-chlorophenyl moiety to occupy the F2 space in the next design.

3. Transformation of the Indole Connection: Indol-3-yl Type. All compounds described above were connected via an indolyl ring at the 1-position with the imidazole moiety. However, taking into consideration the interaction energies between the inhibitors and enzyme, it was considered that a carbon atom was more advantageous in terms of interaction energy than a nitrogen atom in this position. That is, with the unsubstituted indole type, the calculated interaction energies of indol-3-yl and 1-methylindol-3-yl type compounds indicate more stability (ΔE = 1.5 and 2.5 kcal/mol, respectively) than the indol-1-yl type analogues (Table 4). Furthermore, it is well-known in general that the 2-and/or 3-positions of indolyl rings are the main metabolism sites. Although the indol-1-yl type is unprotected from metabolism, in the case of the 1-methylindol-3-yl type, the 3-position of indolyl ring is substituted in addition to the 1- position. So it may be possible to protect from metabolism of the 2- and/or 3-positions of the indolyl ring by hindrance effects, compared to the indol-1-yl type. From this reasoning, we synthesized 1-methylindol-3-yl types (**8a**−**c**) corresponding to the highly potent indol-1-yl types (**6a**,**c**,**e**) (Table 5). The resulting compounds **8b** and **8c** displayed about a 3−4-fold enhancement in inhibitory activity. Compound **8c** showed the best activity for ADA inhibition (K_i = 4.9 nM) among derivatives prepared in these studies (Table 5). Moreover, compound **8c** was also improved in terms of pharmacokinetics compared to the lead compound **1**. That is, compound **8c** showed oral absorption upon administration to rats at 10 mg/kg (C_{max} = 0.21 μg/mL. $AUC_{0-8\ h}$ = 0.26 μg·h/mL, oral bioavailability = 10%).

Table 4. Simulated Interaction Energies for Indol-1-yl and Indol-3-yl Derivatives

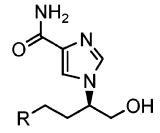

R			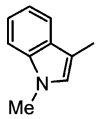
ΔE(kcal/mol)[a]	0.0	-1.5	-2.5

[a] Differential of calculated interaction energies between indol-1-yl and indol-3-yl.

Table 5. Inhibition Constants for Ether-Linked Indol-3-yl Derivatives with ADA

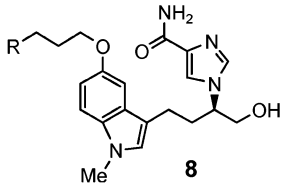

8

compd	R	K_i (nM)[a]
8a	Ph	26
8b	*n*-C_3H_7	13
8c	4-Cl-Ph	4.9

[a] See footnote *a* of Table 1.

4. Chemistry. The amide- and urea-linked compounds listed in Table 1 were synthesized by the routes shown in Scheme 1. Alcohol **10**[25] was converted to mesylate, followed by displacement with 6-nitroindole in the presence of NaH in DMF to afford **11**. Cleavage of the ketal of **11** with 1 N hydrochloric acid (HCl) in THF followed by selective protection of the primary alcohol afforded *tert*-butyldimethylsilyl (TBS) derivative **12**. The secondary alcohol moiety of **12** was then

Scheme 1[a]

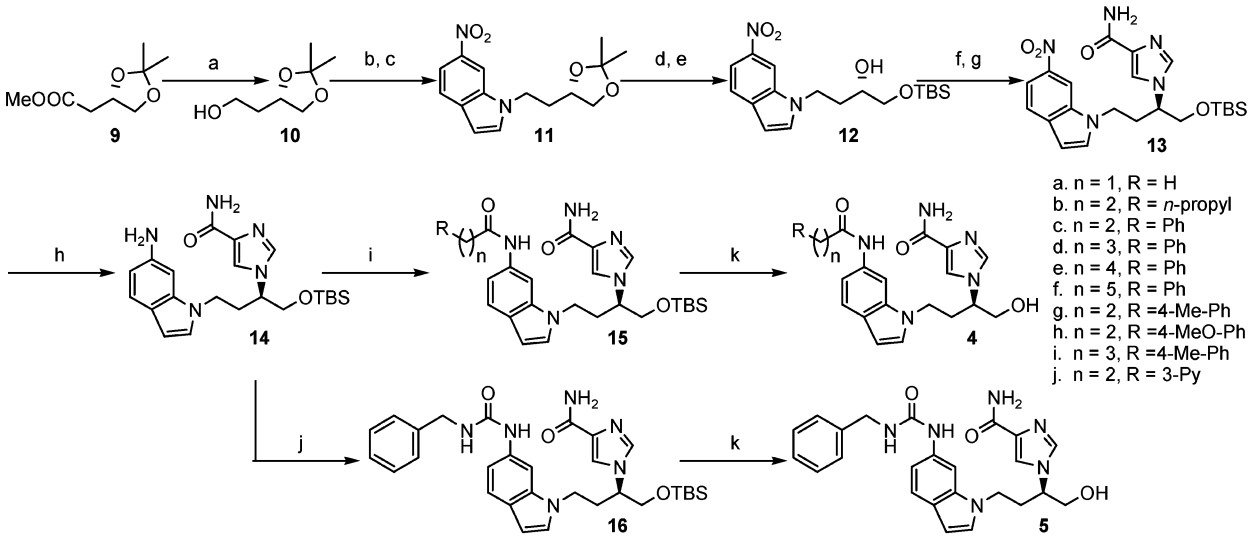

[a] Reagents and conditions: (a) $NaBH_4$, MeOH, 0 °C−rt, 3 h; (b) MsCl, Et_3N, CH_2Cl_2, 0 °C, 1 h; (c) 6-nitroindole, NaH, DMF, 60 °C, 1.5 h; (d) 1 N HCl, THF, 0 °C−rt, 5 h; (e) TBSCl, imidazole, DMF, 0 °C−rt, overnight; (f) MsCl, Et_3N, CH_2Cl_2, 0 °C, 1 h; (g) 4-imidazolecarboxamide, NaH, DMF, 70 °C, 24 h; (h) Fe, NH_4Cl, EtOH-H_2O, 90 °C, 40 min; (i) WSCD·HCl, HOBt, $R(CH_2)_nCOOH$, CH_2Cl_2, rt, 5 h; (j) benzylisocyanate, THF, rt, 2 h; (k) TBAF, THF, 0 °C, 1 h

Scheme 2[a]

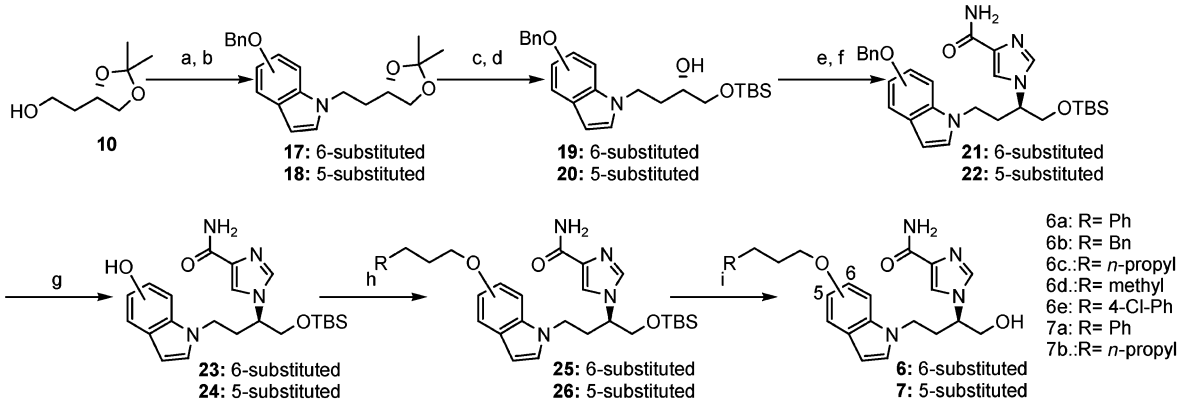

[a] Reagents and conditions: (a) MsCl, Et_3N, CH_2Cl_2, 0 °C, 1 h; (b) 6-benzyloxyindole, NaH, DMF, 60 °C, 1.5 h; (c) 1 N HCl, THF, 0 °C−rt, 5 h; (d) TBSCl, imidazole, DMF, 0 °C-rt, overnight; (e) MsCl, Et_3N, CH_2Cl_2, 0 °C, 1 h; (f) 4-imidazolecarboxamide, NaH, DMF, 70 °C, 24 h; (g) $Pd(OH)_2$, cyclohexene, EtOH, 90 °C, 30 min; (h) 1. $R(CH_2)_3OH$, MsCl, Et_3N, CH_2Cl_2, 0 °C, or $R(CH_2)_3I$; 2. K_2CO_3, DMF, 80-90 °C, 1 day; (i) TBAF, THF, 0 °C, 1 h

converted to mesylate, and displacement by S_N2 reaction with 4-imidazolecarboxamide in the presence of NaH in DMF afforded **13**. Reduction of the nitro group on **13** with iron powder/NH_4Cl in ethanol (EtOH)−H_2O gave the key intermediate aniline **14**. Amides **15a**−**j** or urea **16** were obtained from condensation of **14** with the corresponding carboxylic acid or isocyanate, followed by removal of the TBS group with tetrabutylammonium fluoride (TBAF) to afford **4a**−**j** and **5** in good yields.

The synthetic routes to the ether-linked compounds **6a**−**e** and **7a**,**b** are shown in Scheme 2. Compounds **17**−**22** were prepared by similar procedures to those of compounds **11**, **12**, and **13**, respectively. The key intermediate phenols **23** and **24** were obtained by reductive debenzylation of **21** and **22**, respectively, in the presence of $Pd(OH)_2$ in cyclohexene−EtOH at 90 °C. O-Alkylation of **23** and **24** with the corresponding mesylate or alkyl iodide yielded **25a**−**e** and **26a**,**b**. Deprotection of the TBS group afforded **6a**−**e** and **7a**,**b** in good yields.

The ether-linked 1-methylindol-3-yl derivatives **8a**−**c** were synthesized as shown in Scheme 3. Chain elongation of **27** under Wittig−Horner conditions with triethyl phosphonoacetate in the presence of NaH in DMF yielded **28**. Catalytic hydrogenation with palladium on carbon (Pd−C) in EtOH−THF followed by the reduction of the ester group with diisobutylaluminum hydride (DIBAL-H) in CH_2Cl_2 at −78 °C gave the corresponding aldehyde **30**. Conversion of aldehyde to alkene under Wittig conditions with Ph_3PMeBr in the presence of *n*-butyllithium (*n*-BuLi) in THF yielded **31**. Stereoselective dihydroxylation of **31** was accomplished by Sharpless oxidation with AD-mix-α in *t*-BuOH−H_2O at 0 °C,[26] followed by selective protection of the primary alcohol of **32** to afford **33.** Compounds **34**, **35**, **36**, and **8** were prepared by similar procedures to those of compound **21**, **23**, **25**, and **6**, respectively.

Conclusions

We optimized the novel non-nucleoside ADA inhibitor **1** by a structure-based approach using the crystal structure of the **1**/ADA complex and discovered several new nM potent ADA inhibitors with different structures.

Scheme 3[a]

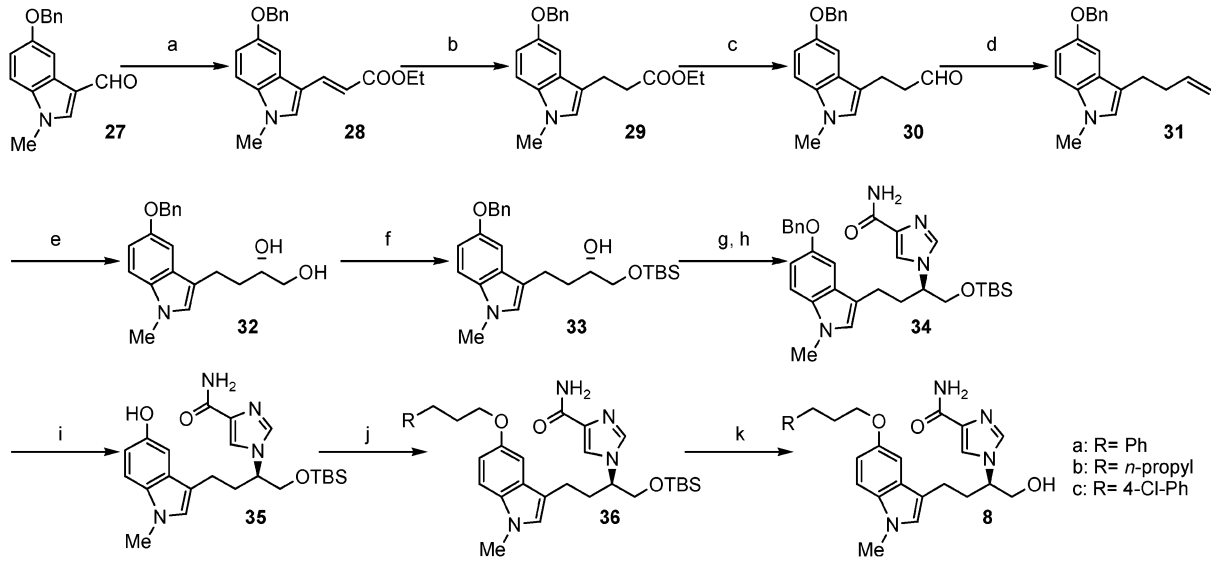

[a] Reagents and conditions: (a) triethyl phosphonacetate, NaH, DMF, 0 °C−rt, overnight; (b) H_2/Pd-C, EtOH−THF, rt, 2.5 h; (c) DIBAL-H, CH_2Cl_2, rt, 30 min; (d) Ph_3PMeBr, *n*-BuLi, THF, -78 °C-rt, 2 h; (e) AD-mix-α, *t*-BuOH−H_2O, 0 °C, 4 h; (f) TBSCl, imidazone, DMF, 0 °C−rt, overnight; (g) MsCl, CH_2Cl_2, 0 °C, 1 h; (h); 4-imidazolecarboxamide, NaH, DMF, 70 °C, 24 h; (i) $Pd(OH)_2$, cyclohexene, EtOH, 90 °C, 30 min; (j) 1. $R(CH_2)_3OH$, MsCl, Et_3N, CH_2Cl_2, 0 °C or $R(CH_2)_3I$; 2. K_2CO_3, DMF, 80-90 °C, 1 day (k) TBAF, THF, 0 °C, 1 h

Furthermore, the SAR of these compounds was revealed in detail by molecular modeling and crystal structure analysis of the complexes. Key points are (1) replacement of the benzimidazole of **1** with a simple aromatic ring and alkyl chains is possible, (2) the permissible distance from the indole moiety to the distal hydrophobic space in the active site was determined, (3) replacement of the amide-linker with urea and ether-linkers was shown to be viable, (4) introduction of substituents (especially chlorine) to the distal phenyl ring is feasible, (5) transformation of indol-1-yl to indol-3-yl improves potency. Consequently, we discovered new structures more amenable to synthetic modification, while retaining potent ADA inhibitory activity. There is currently no other comparable data available for semi-tight-binding inhibitors. The information from this study should be useful for the further design of novel ADA inhibitors. Finally, compound **8c**, a potent inhibitor of ADA, was discovered and found to be orally bioavailable in rats (BA = 10%). The discovery of a potent orally bioavailable ADA inhibitor provides an important tool to further study the biological function of this enzyme and to aid in the development of new medications as antiinflammatory drugs.

Experimental Section

General Methods. Melting points were obtained on a Buchi 535 apparatus and are uncorrected. Infrared (IR) spectra were measured on a HORIBA FT-710 spectrometer. ^{1}H NMR spectra were recorded on a Varian EM-390 NMR spectrometer or a Bruker AC200P spectrometer. Chemical shifts are reported downfield from tetramethylsilane (= 0) for ^{1}H NMR. Mass spectra (MS) were determined on a Hitachi Model M-80 mass spectrometer (EIMS). Optical rotations were measured in absolute ethanol on a HORIBA SEPA-300 polarimeter. Elemental analyses were performed on a Perkin-Elmer 2400 CHN elemental analyzer. Reagents and solvents were used as obtained from commercial suppliers without further purification. Chromatographic purification of the compounds was performed on silica gel 60 (63−200 μm) purchased from Merck Co.

1-[2-((4*S*)-2,2-Dimethyl-1,3-dioxolan-4-yl)ethyl]-1*H*-6-nitroindole (11). To a stirred mixture of 2-[(4*S*)-2,2-dimethyl-1,3-dioxolan-4-yl]ethanol (1.65 g, 11.3 mmol) and methanesulfonyl chloride (MsCl) (1.81 g, 15.8 mmol) in dichloromethane (CH_2Cl_2) (20 mL) was added dropwise triethylamine (Et_3N) (1.60 g, 15.8 mmol) at ice-bath temperature. After 1 h, the reaction mixture was partitioned between CH_2Cl_2 and water. The organic layer was washed with brine, dried ($MgSO_4$), and concentrated in vacuo to give the methanesulfonate (2.60 g) as an oil. This material was used immediately without further purification.

To a solution of 6-nitroindole(1.89 g, 11.3 mmol) in DMF (20 mL) was added NaH (60% in mineral oil, 452 mg, 11.3 mmol) at room temperature. The reaction mixture was stirred for 30 min. A solution of the methanesulfonate prepared above in DMF (8 mL) was added, and the resulting mixture was stirred for 1.5 h at room temperature. The reaction mixture was cooled to 10 °C in an ice bath, and the insoluble material was filtered and washed thoroughly with CH_2Cl_2. The filtrate and washings were combined and then washed with brine. The organic layer was dried ($MgSO_4$) and concentrated in vacuo. The residue was purified by silica gel (40 g) column chromatography eluting with toluene/ethyl acetate (EtOAc) (50:1−20:1) to give **11** (2.19 g, 66.8%) as a yellow solid; IR (KBr, cm^{-1}) 1583, 1074; ^{1}H NMR ($CDCl_3$) δ 1.34 (3H, s), 1.48 (3H, s), 1.90−2.25 (2H, m), 3.45−3.60 (1H, m), 3.85−4.05 (2H, m), 4.41 (2H, dd, J = 7.9 Hz, 5.6 Hz), 6.61 (1H, d, J = 3.1 Hz), 7.42 (1H, d, J = 3.1 Hz), 7.65 (1H, d, J = 8.8 Hz), 8.01 (1H, dd, J = 8.8 Hz, 2.0 Hz), 8.41 (1H, d, J = 2.0 Hz); MS (ESI, m/z) 291 $(M + H)^+$; $[\alpha]^{26}_D$ −9.3 ° (*c* 0.50, EtOH).

(*S*)-[1-(*tert*-Butyldimethylsilyloxy)-4-(6-nitroindol-1-yl)]butan-2-ol (12). To an ice-cooled solution of **11** (1.45 g, 5.00 mmol) in THF (30 mL) was added portionwise 1 N HCl (20 mL). After the addition was completed, the reaction mixture was stirred at room temperature for 5 h. An aqueous solution of $NaHCO_3$ was added, and the resulting mixture was stirred for several minutes. The mixture was extracted with EtOAc. The organic layer was washed with brine, dried ($MgSO_4$), and concentrated in vacuo to give (*S*)-4-(6-nitroindol-1-yl)butane-1,2-diol (1.44 g) as an oil. This material was used immediately without further purification.

To an ice-cooled solution of (*S*)-4-(6-nitroindol-1-yl)butane-1, 2-diol in DMF (20 mL) was added imidazole (1.02 g, 15.0 mmol) followed by *tert*-butyldimethylsilyl chloride (TBSCl) (791 mg, 5.25 mmol). After 30 min, the ice-bath was removed, and

then the mixture was stirred overnight at room temperature. The reaction mixture was poured into water (200 mL) and extracted with EtOAc. The organic layer was washed with brine, dried ($MgSO_4$), and concentrated in vacuo. The residue was purified by silica gel (25 g) column chromatography eluting with hexane/EtOAc (10:1) to give **12** (1.61 g, 88.3%); IR (KBr, cm^{-1}) 3558, 1511; ^1H NMR ($CDCl_3$) δ 0.04 (6H, s), 0.88 (9H, s), 1.80−2.00 (2H, m), 2.51 (1H, d, J = 3.2 Hz), 3.30−3.65 (3H, m), 4.43 (2H, dd, J = 7.7 Hz, 6.0 Hz), 6.59 (1H, d, J = 3.1 Hz), 7.45 (1H, d, J = 3.1 Hz), 7.65 (1H, d, J = 8.8 Hz), 8.01 (1H, dd, J = 8.8 Hz, 2.0 Hz), 8.39 (1H, d, J = 2.0 Hz); MS (ESI, m/z) 365 $(M + H)^+$; $[\alpha]^{26}_D$ −62.0° (c 0.50, EtOH).

1-[(*R*)-1-(*tert*-Butyldimethylsilyloxy)-4-(6-nitroindol-1-yl)-2-butyl]imidazole-4-carboxamide (13). To a stirred mixture of **12** (1.53 g, 4.21 mmol) and methanesulfonyl chloride (675 mg, 5.89 mmol) in CH_2Cl_2 (30 mL) was added dropwise Et_3N (596 mg, 5.89 mmol) at ice-bath temperature. After 1 h, the reaction mixture was partitioned between CH_2Cl_2 and water. The organic layer was washed with brine, dried ($MgSO_4$), and concentrated in vacuo to give the methanesulfonate (1.84 g) as an oil. This material was used for the next reaction without further purification.

To a solution of 4-imidazolecarboxamide (467 mg, 4.21 mmol) in DMF (10 mL) was added NaH (60% in mineral oil, 194 mg, 4.84 mmol) at room temperature. The reaction mixture was stirred for 1 h at 70 °C. The methanesulfonate prepared above was added, and the resulting mixture was stirred for 38 h at 70 °C. The reaction mixture was cooled to 10 °C in an ice bath, and the insoluble material was filtered and washed thoroughly with CH_2Cl_2. The filtrate and washings were combined and washed with brine. The organic layer was dried (Na_2SO_4) and concentrated in vacuo. The residue was purified by silica gel (66 g) column chromatography eluting with chloroform ($CHCl_3$)/methanol (MeOH) (30:1) to give **13** (489 mg, 25.4%); IR (KBr, cm^{-1}) 3600−3000, 1662, 1504; ^1H NMR ($CDCl_3$) δ −0.08 (3H, s), −0.06 (3H, s), 0.81 (9H, s), 2.25−2.65 (2H, m), 3.65−4.20 (5H, m), 5.44 (1H, brs), 6.62 (1H, d, J = 3.1 Hz), 6.97 (1H, brs), 7.16 (1H, d, J = 3.1 Hz), 7.40 (1H, s), 7.66 (1H, s), 7.68 (1H, d, J = 8.8 Hz), 8.04 (1H, dd, J = 8.8 Hz, 2.0 Hz), 8.18 (1H, d, J = 2.0 Hz); MS (ESI, m/z) 458 $(M + H)^+$; $[\alpha]^{27}_D$ −3.3° (c 0.50, EtOH).

1-[(*R*)-4-(6-Aminoindol-1-yl)-1-(*tert*-butyldimethylsilyloxy)-2-butyl]imidazole-4-carboxamide (14). To a mechanically stirred mixture of **13** (450 mg, 0.98 mmol) and ammonium chloride (45 mg) in EtOH (10 mL) and water (5 mL) was added portionwise iron powder (450 mg) at 90 °C. The resulting mixture was stirred for 40 min at 90 °C. After cooling, the insoluble material was filtered through Celite and washed with ethanol and ethyl acetate. The filtrate and washings were combined and concentrated in vacuo. The resulting residue was extracted with EtOAc and washed with brine. The organic layer was dried (Na_2SO_4) and concentrated in vacuo to give **14** (397 mg, 94.7%). This material was used for the next reaction without further purification. IR (KBr, cm^{-1}) 3700−3000, 1662, 1627; ^1H NMR ($CDCl_3$) δ −0.10 (3H, s), −0.08 (3H, s), 0.81 (9H, s), 2.00−2.70 (4H, br), 3.60−4.15 (5H, m), 5.44 (1H, brs), 6.36 (1H, d, J = 1.9 Hz), 6.38 (1H, d, J = 3.2 Hz), 6.57 (1H, dd, J = 8.3 Hz, 1.9 Hz), 6.71 (1H, d, J = 3.2 Hz), 7.00 (1H, brs), 7.39 (1H, d, J = 8.3 Hz), 7.41 (1H, s), 7.68 (1H, s); MS (ESI, m/z) 428 $(M + H)^+$.

1-[(*R*)-1-(*tert*-Butyldimethylsilyloxy)-4-(6-(3-phenylpropionylamino)indol-1-yl)-2-butyl]-imidazole-4-carboxamide (15c). To a stirred mixture of 3-phenylpropionic acid (46 mg, 0.304 mmol) and 1-hydroxybenzotriazole (45 mg, 0.334 mmol) in CH_2Cl_2 (5 mL) was added 1-(3-dimethylaminopropyl)-3-ethylcarbodiimide (52 mg, 0.334 mmol) at ice-bath temperature. The mixture was stirred for 40 min at room temperature, and then **14** (130 mg, 0.304 mmol) was added to the mixture at ice-bath temperature. After addition, the resulting mixture was stirred for 4 h at room temperature. The solvent was concentrated in vacuo, and the residue extracted with ethyl acetate and washed with water and brine. The organic layer was dried (Na_2SO_4) and concentrated in vacuo. The residue was purified by silica gel (6 g) column chromatography eluting with $CHCl_3$/MeOH(30:1) to give **15c** (170.6 mg, 100%); IR (KBr, cm^{-1}) 3600−3000, 1660; ^1H NMR ($CDCl_3$) δ −0.10 (3H, s), −0.08 (3H, s), 0.81 (9H, s), 2.20−2.55 (2H, m), 2.73 (2H, t, J = 7.6 Hz), 3.10 (2H, t, J = 7.6 Hz), 3.60−4.25 (5H, m), 5.42 (1H, brs), 6.45 (1H, d, J = 3.1 Hz), 6.86 (1H, d, J = 3.1 Hz), 6.90−7.05 (2H, m), 7.15−7.35 (5H, m), 7.40−7.65 (5H, m); MS (ESI, m/z) 560 $(M + H)^+$.

1-[(*R*)-1-Hydroxy-4-(6-(3-phenylpropionylamino)indol-1-yl)-2-butyl]imidazole-4-carboxamide (4c). To an ice-cooled solution of **15c** (150 mg, 0.268 mmol) in THF (5 mL) was added dropwise 1.0 M TBAF in THF (402 μL). After the addition was completed, the reaction mixture was stirred at ice-bath temperature for 30 min. 25% $AcONH_4$ (4 mL) was added, and the resulting mixture was stirred for several minutes and then extracted with EtOAc. The organic layer was washed with brine, dried (Na_2SO_4), and concentrated in vacuo. The residue was purified by silica gel (6 g) column chromatography eluting with $CHCl_3$/MeOH (10:1) to give **4c** (96.6 mg, 80.9%) as a white solid; mp 97−100 °C; IR (KBr, cm^{-1}) 3700−2800, 1656; ^1H NMR (DMSO-d_6) δ 2.20−2.40 (2H, m), 2.63 (2H, t, J = 7.5 Hz), 2.94 (2H, t, J = 7.5 Hz), 3.60 (2H, t, J = 5.2 Hz), 3.80−4.20 (3H, m), 5.07 (1H, t, J = 5.2 Hz), 6.36 (1H, d, J = 3.0 Hz), 6.95−7.35 (9H, m), 7.43 (1H, d, J = 8.3 Hz), 7.65−7.90 (3H, m), 9.86 (1H, brs); MS (ESI, m/z) 446 $(M + H)^+$; $[\alpha]^{24}_D$ +18.0° (c 0.50, EtOH); Anal. ($C_{25}H_{27}N_5O_3 \cdot 0.5H_2O$) C, H, N.

1-[(*R*)-1-(*tert*-Butyldimethylsilyloxy)-4-(6-acetylaminoindol-1-yl)-2-butyl]imidazole-4-carboxamide (15a). Replacing 3-phenylpropionic acid with acetic acid and following the same procedure as in the preparation of **15c** gave **15a** (69.4 mg, 90.3%). IR (KBr, cm^{-1}) 3600−3000, 1664; ^1H NMR ($CDCl_3$) δ −0.10 (3H, s), −0.08 (3H, s), 0.80 (9H, s), 2.23 (3H, s), 2.30−2.50 (2H, m), 3.60−4.20 (5H, m), 5.51 (1H, brs), 6.46 (1H, d, J = 3 Hz), 6.88 (1H, d, J = 3 Hz), 7.00−7.15 (2H, m), 7.40−7.75 (5H, m); MS (ESI, m/z) 470 $(M + H)^+$; $[\alpha]^{26}_D$ +16.3° (c 0.50, EtOH).

1-[(*R*)-4-(6-Acetylaminoindol-1-yl)-1-hydroxy-2-butyl]-imidazole-4-carboxamide (4a). To an ice-cooled solution of **15a** (62 mg, 0.133 mmol) in THF (5 mL) was added dropwise 1.0 M TBAF in THF (199 μL). After addition, the reaction mixture was stirred at ice-bath temperature for 1 h. 25% $AcONH_4$ (5 mL) was added, and the resulting mixture was stirred for several minutes and then extracted with water. Because of high water solubility of **4a**, the aqueous layer was washed with EtOAc and was purified by HP-20 (15 cm^3) column chromatography eluting with water/2-propanol (IPA) (9:1) and lyophilized to give **4a** (41 mg, 86.8%) as an amorphous solid. IR (KBr, cm^{-1}) 3600−3000, 1662; ^1H NMR (DMSO-d_6) δ 2.05 (3H, s), 2.20−2.40 (2H, m), 3.50−4.20 (5H, m), 5.11 (1H, brs), 6.36 (1H, d, J = 3 Hz), 7.00−7.15 (2H, m), 7.17 (1H, d, J = 3 Hz), 7.30 (1H, brs) 7.43 (1H, d, J = 9 Hz), 7.70−7.85 (3H, m), 9.89 (1H, brs); MS (ESI, m/z) 356 $(M + H)^+$; $[\alpha]^{27}_D$ +13.6° (c 0.50, MeOH); Anal. ($C_{18}H_{21}N_5O_3 \cdot 0.5IPA \cdot 1.0H_2O$) C, H, N.

1-[(*R*)-1-(*tert*-Butyldimethylsilyloxy)-4-(6-hexanoylaminoindol-1-yl)-2-butyl]imidazole-4-carboxamide (15b). Replacing 3-phenylpropionic acid with hexanoic acid and following the same procedure as in the preparation of **15c** gave **15b** (149 mg, 93.2%). IR (KBr, cm^{-1}) 3600−3000, 1660; ^1H NMR ($CDCl_3$) δ −0.10 (3H, s), −0.08 (3H, s), 0.80 (9H, s), 0.93 (3H, t, J = 6.6 Hz), 1.30−1.50 (4H, m), 1.70−1.90 (2H, m), 2.20−2.50 (4H, m), 3.60−4.25 (5H, m), 5.43 (1H, brs), 6.45 (1H, d, J = 3.1 Hz), 6.84 (1H, d, J = 3.1 Hz), 6.95−7.10 (2H, m), 7.45−7.60 (3H, m), 7.63 (1H, s), 7.75 (1H, s); MS (ESI, m/z) 526 $(M + H)^+$; $[\alpha]^{24}_D$ +19.9° (c 0.50, EtOH).

1-[(*R*)-4-(6-Hexanoylaminoindol-1-yl)-1-hydroxy-2-butyl]imidazole-4-carboxamide (4b). Replacing **15c** with **15b** and following the same procedure as in the preparation of **4c** gave **4b** (89.9 mg, 79.7%) as an amorphous solid. IR (KBr, cm^{-1}) 3600−3000, 1656; ^1H NMR ($CDCl_3$) δ 0.89 (3H, t, J = 6.5 Hz), 1.20−1.45 (4H, m), 1.61 (2H, qui, J = 7.0 Hz), 2.20−2.40 (4H, m), 3.60 (2H, t, J = 5.2 Hz), 3.85−4.25 (3H, m), 5.06 (1H, t, J = 5.2 Hz), 6.35 (1H, d, J = 3.1 Hz), 7.00−7.15 (2H, m), 7.16 (1H, d, J = 3.1 Hz), 7.29 (1H, brs), 7.42 (1H, d, J =

8.5 Hz), 7.74 (1H, s), 7.78 (1H, s), 7.84 (1H, s), 9.80 (1H, brs); MS (ESI, *m*/*z*) 412 $(M + H)^+$; $[\alpha]^{26}_D$ +25.8° (*c* 0.50, EtOH); Anal. ($C_{22}H_{29}N_5O_3 \cdot 0.25IPE \cdot 0.5H_2O$) C, H, N.

1-[(*R*)-1-(*tert*-Butyldimethylsilyloxy)-4-(6-(4-phenylbutyrylamino)indol-1-yl)-2-butyl]imidazole-4-carboxamide (15d). Replacing 3-phenylpropionic acid with 4-phenylbutyric acid and following the same procedure as in the preparation of **15c** gave **15d** (170.6 mg, 100%). IR (KBr, cm^{-1}) 3600−3000, 1662; ^1H NMR ($CDCl_3$) δ −0.10 (3H, s), −0.08 (3H, s), 0.80 (9H, s), 2.00−2.20 (2H, m), 2.20−2.50 (4H, m), 2.75 (2H, t, J = 7.4 Hz), 3.60−4.25 (5H, m), 5.34 (1H, brs), 6.45 (1H, d, J = 3.2 Hz), 6.86 (1H, d, J = 3.2 Hz), 6.90−7.10 (2H, m), 7.15−7.40 (5H, m), 7.40−7.70 (5H, m); MS (ESI, *m*/*z*) 574 $(M + H)^+$; $[\alpha]^{23}_D$ +15.1° (*c* 0.50, EtOH).

1-[(*R*)-1-Hydroxy-4-(6-(4-phenylbutyrylamino)indol-1-yl)-2-butyl]imidazole-4-carboxamide (4d). Replacing **15c** with **15d** and following the same procedure as in the preparation of **4c** gave **4d** (73.4 mg, 68.4%) as an amorphous solid. IR (KBr, cm^{-1}) 3600−3000, 1656; ^1H NMR (DMSO-d_6) δ 1.80−2.05 (2H, m), 2.15−2.40 (4H, m), 2.64 (2H, t, J = 7.5 Hz), 3.59 (2H, t, J = 5.2 Hz), 3.80−4.20 (3H, m), 5.06 (1H, t, J = 5.2 Hz), 6.36 (1H, d, J = 3.0 Hz), 6.95−7.40 (9H, m), 7.43 (1H, d, J = 8.5 Hz), 7.70−7.90 (3H, m), 9.82 (1H, brs); MS (ESI, *m*/*z*) 460 $(M + H)^+$; $[\alpha]^{24}_D$ +19.0° (*c* 0.50, EtOH); Anal. ($C_{26}H_{29}N_5O_3 \cdot 0.5H_2O$) C, H, N.

1-[(*R*)-1-(*tert*-Butyldimethylsilyloxy)-4-(6-(5-phenylvalerylamino)indol-1-yl)-2-butyl]imidazole-4-carboxamide (15e). Replacing 3-phenylpropionic acid with 5-phenylvaleric acid and following the same procedure as in the preparation of **15c** gave **15e** (82.4 mg, 100%). IR (KBr, cm^{-1}) 3600−3000, 1664; ^1H NMR ($CDCl_3$) δ −0.10 (3H, s), −0.08 (3H, s), 0.80 (9H, s), 1.60−1.95 (4H, m), 2.20−2.55 (4H, m), 2.69 (2H, t, J = 7.0 Hz), 3.60−4.25 (5H, m), 5.37 (1H, brs), 6.45 (1H, d, J = 3.2 Hz), 6.85 (1H, d, J = 3.2 Hz), 6.90−7.10 (2H, m), 7.10−7.35 (5H, m), 7.40−7.60 (3H,m), 7.70 (1H, s), 7.78 (1H, s); MS (ESI, *m*/*z*) 588 $(M + H)^+$; $[\alpha]^{21}_D$ +16.6° (*c* 0.50, EtOH).

1-[(*R*)-1-Hydroxy-4-(6-(5-phenylvalerylamino)indol-1-yl)-2-butyl]imidazole-4-carboxamide (4e). Replacing **15c** with **15e** and following the same procedure as in the preparation of **4c** gave **4e** (54.1 mg, 70.3%) as an amorphous solid. IR (KBr, cm^{-1}) 3600−3000, 1664, 1656; ^1H NMR (DMSO-d_6) δ 1.50−1.75 (4H, m), 2.10−2.45 (4H, m), 2.50−2.75 (2H, m), 3.59 (2H, t, J = 5.2 Hz), 3.80−4.20 (3H, m), 5.06 (1H, t, J = 5.2 Hz), 6.36 (1H, d, J = 2.8 Hz), 6.95−7.35 (9H, m), 7.43 (1H, d, J = 8.5 Hz), 7.70−7.90 (3H, m), 9.82 (1H, brs); MS (ESI, *m*/*z*) 474 $(M + H)^+$; $[\alpha]^{27}_D$ +19.0° (*c* 0.50, EtOH); Anal. ($C_{27}H_{31}N_5O_3 \cdot 0.5H_2O$) C, H, N.

1-[(*R*)-1-(*tert*-Butyldimethylsilyloxy)-4-(6-(6-phenylhexanoylamino)indol-1-yl)-2-butyl]imidazol-4-carboxamide (15f). Replacing 3-phenylpropionic acid with 6-phenylhexanic acid and following the same procedure as in the preparation of **15c** gave **15f** (73.7 mg, 74.8%). IR (KBr, cm^{-1}) 3600−3000, 1658; ^1H NMR($CDCl_3$) δ −0.10 (3H, s), −0.08 (3H, s), 0.80 (9H, s), 1.40−1.95 (6H, m), 2.20−2.50 (4H, m), 2.64 (2H, t, J = 8 Hz), 3.55−4.25 (5H, m), 5.42 (1H, brs), 6.45 (1H, d, J = 3 Hz), 6.85 (1H, d, J = 3 Hz), 6.90−7.35 (7H, m), 7.45−7.75 (5H, m); MS (ESI, *m*/*z*) 602 $(M + H)^+$; $[\alpha]^{23}_D$ +15.9° (*c* 0.50, EtOH).

1-[(*R*)-1-Hydroxy-4-(6-(6-phenylhexanoylamino)indol-1-yl)-2-butyl]imidazole-4-carboxamide (4f). Replacing **15c** with **15f** and following the same procedure as in the preparation of **4c** gave **4f** (47 mg, 86.6%) as an amorphous solid. IR (KBr, cm^{-1}) 3700−3000, 1657; ^1H NMR (DMSO-d_6) δ 1.20−1.75 (6H, m), 2.20−2.70 (6H, m), 3.50−4.20 (5H, m), 5.06 (1H, brs), 6.36 (1H, d, J = 3 Hz), 7.00−7.35 (9H, m), 7.43 (1H, d, J = 9 Hz), 7.70−7.90 (3H, m), 9.80 (1H, brs); MS (ESI, *m*/*z*) 488 $(M + H)^+$; $[\alpha]^{27}_D$ +20.5° (*c* 0.50, EtOH); Anal. ($C_{28}H_{33}N_5O_3 \cdot 0.25H_2O$) C, H, N.

1-[(*R*)-1-(*tert*-Butyldimethylsilyloxy)-4-(6-(3-(4-methylphenyl)propionylamino)indol-1-yl)-2-butyl]imidazole-4-carboxamide (15g). Replacing 3-phenylpropionic acid with 3-(4-methylphenyl)propionic acid and following the same procedure as in the preparation of **15c** gave **15g** (103 mg, 80.7%). IR (KBr, cm^{-1}) 3600−3000, 1664; ^1H NMR ($CDCl_3$) δ −0.10 (3H, s), −0.08 (3H, s), 0.81 (9H, s), 2.20−2.55 (5H, m), 2.71 (2H, t, J = 7.6 Hz), 3.05 (2H, t, J = 7.6 Hz), 3.60−4.20 (5H, m), 5.42 (1H, brs), 6.45 (1H, d, J = 3.0 Hz), 6.85 (1H, d, J = 3.0 Hz), 6.90−7.25 (6H, m), 7.40−7.70 (5H, m); MS (ESI, *m*/*z*) 574 $(M + H)^+$; $[\alpha]^{26}_D$ +16.4° (*c* 0.50, EtOH).

1-[(*R*)-1-Hydroxy-4-(6-(3-(4-methylphenyl)propionylamino)indol-1-yl)-2-butyl]imidazole-4-carboxamide (4g). Replacing **15c** with **15g** and following the same procedure as in the preparation of **4c** gave **4g** (71 mg, 92.5%) as an amorphous solid. IR (KBr, cm^{-1}) 3600−3000, 1656; ^1H NMR (DMSO-d_6) δ 2.10−2.40 (5H, m), 2.60 (2H, t, J = 7.5 Hz), 2.89 (2H, t, J = 7.5 Hz), 3.61 (2H, t, J = 5.2 Hz), 3.85−4.25 (3H, m), 5.08 (1H, brs), 6.36 (1H, d, J = 3.0 Hz), 6.95−7.25 (7H, m), 7.41 (1H, brs), 7.43 (1H, d, J = 8.5 Hz), 7.70−8.00 (3H, m), 9.84 (1H, brs); MS (ESI, *m*/*z*) 460$(M + H)^+$; $[\alpha]^{27}_D$ +11.9° (*c* 0.50, EtOH); Anal. ($C_{26}H_{29}N_5O_3 \cdot 0.8H_2O$) C, H, N.

1-[(*R*)-1-(*tert*-Butyldimethylsilyloxy)-4-(6-(3-(4-methoxylphenyl)propionylamino)indol-1-yl)-2-butyl]imidazole-4-carboxamide (15h). Replacing 3-phenylpropionic acid with 3-(4-methoxylphenyl)propionic acid and following the same procedure as in the preparation of **15c** gave **15h** (105 mg, 80.2%). IR (KBr, cm^{-1}) 3600−3000, 1664, 1247; ^1H NMR ($CDCl_3$) δ −0.10 (3H, s), −0.08 (3H, s), 0.81 (9H, s), 2.20−2.55 (2H, m), 2.69 (2H, t, J = 7.6 Hz), 3.04 (2H, t, J = 7.6 Hz), 3.55−4.25 (10H, m), 5.44 (1H, brs), 6.45 (1H, d, J = 3.0 Hz), 6.75−7.05 (5H, m), 7.15−7.25 (2H, m), 7.40−7.65 (5H, m); MS (ESI, *m*/*z*) 590 $(M + H)^+$; $[\alpha]^{27}_D$ +16.8° (*c* 0.50, EtOH).

1-[(*R*)-1-Hydroxy-4-(6-(3-(4-methoxylphenyl)propionylamino)indol-1-yl)-2-butyl]imidazole-4-carboxamide (4h). Replacing **15c** with **15h** and following the same procedure as in the preparation of **4c** gave **4h** (67 mg, 85.6%) as an amorphous solid. IR (KBr, cm^{-1}) 3700−3000, 1656, 1241; ^1H NMR(DMSO-d_6) δ 2.20−2.40 (2H, m), 2.59 (2H, t, J = 7.5 Hz), 2.87 (2H, t, J = 7.5 Hz), 3.60 (2H, t, J = 5.2 Hz), 3.71 (3H, S), 3.90−4.20 (3H, m), 5.06 (1H, t, J = 5.2 Hz), 6.36 (1H, d, J = 3.0 Hz), 6.85 (2H, d, J = 8.6 Hz), 7.00−7.25 (5H, m), 7.28 (1H, brs), 7.43 (1H, d, J = 8.5 Hz), 7.70−7.90 (3H, m), 9.83 (1H, brs); MS (ESI, *m*/*z*) 476 $(M + H)^+$; $[\alpha]^{28}_D$ +17.1° (*c* 0.50, EtOH); Anal. ($C_{26}H_{29}N_5O_4 \cdot 0.6H_2O$) C, H, N.

1-[(*R*)-1-(*tert*-Butyldimethylsilyloxy)-4-(6-(4-(4-methylphenyl)butyrylamino)indol-1-yl)-2-butyl]imidazole-4-carboxamide (15i). Replacing 3-phenylpropionic acid with 4-(4-methylphenyl)butyric acid and following the same procedure as in the preparation of **15c** gave **15i** (103 mg, 78.9%). IR (KBr, cm^{-1}) 3600−3000, 1664; ^1H NMR ($CDCl_3$) δ −0.10 (3H, s), −0.08 (3H, s), 0.80 (9H, s), 1.95−2.20 (2H, m), 2.20−2.50 (7H, m), 2.71 (2H, t, J = 7.4 Hz), 3.50−4.25 (5H, m), 5.37-(1H, brs), 6.45 (1H, d, J = 3.0 Hz), 6.85 (1H, d, J = 3.0 Hz), 6.90−7.20 (6H, m), 7.40−7.70 (5H, m); MS (ESI, *m*/*z*) 588 (M + H)$^+$; $[\alpha]^{25}_D$ +14.7° (*c* 0.50, EtOH).

1-[(*R*)-1-Hydroxy-4-(6-(4-(4-methylphenyl)butyrylamino)indol-1-yl)-2-butyl]imidazole-4-carboxamide (4i). Replacing **15c** with **15i** and following the same procedure as in the preparation of **4c** gave **4i** (63.8 mg, 82.5%) as an amorphous solid. IR (KBr, cm^{-1}) 3700−3000, 1656; ^1H NMR (DMSO-d_6) δ 1.80−2.00 (2H, m), 2.20−2.40 (7H, m), 2.60 (2H, t, J = 7.5 Hz), 3.60 (2H, d, J = 5.2 Hz), 3.90−4.25 (3H, m), 5.08 (1H, brs), 6.36 (1H, d, J = 3.0 Hz), 7.00−7.25 (7H, m), 7.40 (1H, brs), 7.42 (1H, d, J = 8.5 Hz), 7.75−8.00 (3H, m), 9.81 (1H, brs); MS (ESI, *m*/*z*) 474 $(M + H)^+$; $[\alpha]^{27}_D$ +13.0° (*c* 0.50, EtOH); Anal. ($C_{27}H_{31}N_5O_3 \cdot 1.0H_2O$) C, H, N.

1-{(*R*)-1-(*tert*-Butyldimethylsilyloxy)-4-[6-(3-(3-pyridyl)propionylamino)indol-1-yl]-2-butyl}imidazole-4-carboxamide (15j). Replacing 3-phenylpropionic acid with 3-(3-pyridyl)propionic acid and following the same procedure as in the preparation of **15c** gave **15j** (103 mg, 82.8%). IR (KBr, cm^{-1}) 3600−3000, 1664; ^1H NMR ($CDCl_3$) δ −0.09 (3H, s), −0.07 (3H, s), 0.81 (9H, s), 2.20−2.50 (2H, m), 2.76 (2H, t, J = 8 Hz), 3.11 (2H, t, J = 8 Hz), 3.55−4.20 (5H, m), 5.46 (1H, brs), 6.46 (1H, d, J = 3 Hz), 6.89 (1H, d, J = 3 Hz), 7.00 (1H, brs), 7.10−7.30 (2H, m), 7.40−7.70 (5H, m), 7.89 (1H, brs), 8.40−8.60 (2H, m); MS (ESI, *m*/*z*) 561 $(M + H)^+$; $[\alpha]^{26}_D$ +13.3° (*c* 0.50, EtOH).

1-{(*R*)-1-Hydroxy-4-[6-(3-(3-pyridyl)propionylamino)-indol-1-yl]-2-butyl}imidazole-4-carboxamide (4j). Replacing **15a** with **15j** and following the same procedure as in the preparation of **4a** gave **4j** (73.4 mg, 97.2%) as an amorphous solid. IR (KBr, cm^{-1}) 3600−2800, 1664; ^1H NMR (DMSO-d_6) δ 2.20−2.40 (2H, m), 2.67 (2H, t, J = 8 Hz), 2.95 (2H, t, J = 8 Hz), 3.50−4.25 (5H, m), 5.09 (1H, brs), 6.36 (1H, d, J = 3 Hz), 7.00−7.16 (2H, m), 7.18 (1H, d, J = 3 Hz), 7.20−7.40 (2H, m), 7.43 (1H, d, J = 9 Hz), 7.65−7.90 (4H, m), 8.30−8.55 (2H, m), 9.87 (1H, brs); MS (ESI, m/z) 447 (M + H)$^+$; $[\alpha]^{27}_D$ +12.4 ° (c 0.40, EtOH); Anal. ($C_{24}H_{26}N_6O_3$·0.5IPA·1.0H_2O) C, H, N.

1-[(*R*)-4-(6-(3-Benzylureido)indol-1-yl)-1-(*tert*-butyldimethylsilyloxy)-2-butyl]imidazole-4-carboxamide (16). To a solution of **14** (100 mg, 0.234 mmol) in THF (5 mL) was added dropwise benzyl isocyanate (32 μL, 0.257 mmol). The reaction mixture was stirred at room temperature for 2 h and the solvent was concentrated in vacuo. The residue was purified by silica gel (4.5 g) column chromatography eluting with $CHCl_3$/MeOH (30:1) to give **16** (101 mg, 77%) as a pale yellow solid. IR (KBr, cm^{-1}) 3600−3000, 1654; ^1H NMR ($CDCl_3$) δ −0.10 (3H, s), −0.08 (3H, s), 0.81 (9H, s), 2.20−2.40 (2H, m), 3.55−4.10 (5H, m), 4.47 (2H, d, J = 6 Hz), 5.39 (1H, brs), 5.66 (1H, t, J = 6 Hz), 6.44 (1H, d, J = 3 Hz), 6.85−6.92 (2H, m), 7.01 (1H, brs), 7.15−7.40 (7H, m), 7.40−7.65 (3H, m); MS (ESI, m/z) 561 (M + H)$^+$; $[\alpha]^{26}_D$ +17.9° (c 0.50, EtOH).

1-[(*R*)-4-(6-(3-Benzylureido)indol-1-yl)-1-hydroxy-2-butyl]imidazole-4-carboxamide (5). Replacing **15c** with **16** and following the same procedure as in the preparation of **4c** gave **5** (75 mg, 98.2%) as an amorphous solid. IR (KBr, cm^{-1}) 3600−2800, 1654; ^1H NMR (DMSO-d_6) δ 2.15−2.40 (2H, m), 3.59 (2H, t, J = 5 Hz), 3.85−4.20 (3H, m), 4.32 (2H, d, J = 6 Hz), 5.05 (1H, t, J = 5 Hz), 6.32 (1H, d, J = 3 Hz), 6.56 (1H, t, J = 6 Hz), 6.90 (1H, dd, J = 8 Hz, 2 Hz), 6.95−7.45 (9H, m), 7.62 (1H, d, J = 2 Hz), 7.73 (1H, s), 7.79 (1H, s), 8.46 (1H, s); MS (ESI, m/z) 447 (M + H)$^+$; $[\alpha]^{24}_D$ +10.0° (c 0.20, MeOH); Anal. ($C_{24}H_{26}N_6O_3$·1.0H_2O) C, H, N.

1-[(*R*)-1-(*tert*-Butyldimethylsilyloxy)-4-(6-hydroxyindol-1-yl)-2-butyl]imidazole-4-carboxamide (23). To a solution of **21** (975 mg, 1.88 mmol) in cyclohexene (10 mL) and EtOH (20 mL) was added 20% palladium hydroxide on carbon (488 mg). The resulting mixture was stirred at reflux for 1 h. After cooling to room temperature, the mixture was filtered through Celite and washed with EtOH. The filtrate was concentrated in vacuo and the residue purified by silica gel (20 g) chromatography eluting with $CHCl_3$/MeOH (100:1 to 50:1) to give **23** (772 mg, 95.8%) as a colorless solid. IR (KBr, cm^{-1}) 3700−3000, 1658, 1255; ^1H NMR ($CDCl_3$) δ −0.09 (3H, s), −0.07 (3H, s), 0.81 (9H, s), 2.20−2.55 (2H, m), 3.55−4.05 (5H, m), 5.64 (1H, brs), 6.43 (1H, d, J = 3 Hz), 6.56 (1H, d, J = 2 Hz), 6.74 (1H, dd, J = 8 Hz, 2 Hz), 6.81 (1H, d, J = 3 Hz), 7.06 (1H, brs), 7.44 (1H, d, J = 8 Hz), 7.46 (1H, s), 7.73 (1H, s); MS (ESI, m/z) 429 (M + H)$^+$; $[\alpha]^{26}_D$ +25.7° (c 0.50, EtOH).

1-[(*R*)-1-(*tert*-Butyldimethylsilyloxy)-4-(6-(3-phenylpropoxy)indol-1-yl)-2-butyl]imidazole-4-carboxamide (25a). To a stirred mixture of 3-phenylpropanol (40 mg, 0.294 mmol) and MsCl (40 mg, 0.353 mmol) in CH_2Cl_2 (5 mL) was added dropwise Et_3N (36 mg, 0.353 mmol) at ice-bath temperature. After 1 h, the reaction mixture was partitioned between CH_2Cl_2 and water. The organic layer was washed with brine, dried ($MgSO_4$), and concentrated in vacuo to give the methanesulfonate (62.7 mg, 100%) as an oil. This material was used immediately without further purification.

Under N_2 atmosphere, to a solution of **23** (80 mg, 0.187 mmol) in DMF (4 mL) was added potassium carbonate (38.7 mg, 0.280 mmol) at room temperature. The reaction mixture was stirred for 20 min, the methanesulfonate prepared above in DMF (2 mL) was then added, and the resulting mixture was stirred for 24 h at 80 to 90 °C. The reaction mixture was poured into water (20 mL) and extracted with EtOAc. The extract was washed with brine, dried (Na_2SO_4), and evaporated in vacuo. The residue was purified by silica gel (4 g) chromatography eluting with $CHCl_3$/MeOH (100:1 to 10:1) to give **25a** (93.6 mg, 81.5%). IR (neat, cm^{-1}) 3600−3000, 1666, 1250; ^1H NMR ($CDCl_3$) δ −0.10 (3H, s), −0.08 (3H, s), 0.80 (9H, s), 2.00−2.60 (4H, m), 2.86 (2H, t, J = 8 Hz), 3.60−4.20 (7H, m), 5.40 (1H, brs), 6.44 (1H, d, J = 3 Hz), 6.56 (1H, d, J = 2 Hz), 6.78 (1H, d, J = 3 Hz), 6.80 (1H, dd, J = 9 Hz, 2 Hz), 6.95 (1H, brs), 7.10−7.35 (5H, m), 7.38 (1H, s), 7.49 (1H, d, J = 9 Hz), 7.67 (1H, s); MS (ESI, m/z) 547 (M + H)$^+$; $[\alpha]^{28}_D$ +8.6° (c 0.50, EtOH).

1-[(*R*)-1-Hydroxy-4-(6-(3-phenylpropoxy)indol-1-yl)-2-butyl]imidazole-4-carboxamide (6a). Replacing **15c** with **25a** and following the same procedure as in the preparation of **4c** gave **6a** (55.6 mg, 78.1%) as a white solid; mp 135−136 °C; IR (KBr, cm^{-1}) 3319, 3186, 1680, 1238; ^1H NMR (DMSO-d_6) δ 1.90−2.40 (4H, m), 2.78 (2H, t, J = 8 Hz), 3.60 (2H, t, J = 5 Hz), 3.80−4.20 (5H, m), 5.04 (1H, t, J = 5 Hz), 6.34 (1H, d, J = 3 Hz), 6.68 (1H, dd, J = 9 Hz, 2 Hz), 6.73 (1H, d, J = 2 Hz), 7.00−7.45 (9H, m), 7.70 (1H, s), 7.80(1H, s); MS (ESI, m/z) 433(M + H)$^+$; $[\alpha]^{27}_D$ +16.3° (c 0.50, MeOH); Anal. ($C_{25}H_{28}N_4O_3$) C, H, N.

1-[(*R*)-1-(*tert*-Butyldimethylsilyloxy)-4-(6-(4-phenylbutoxy)indol-1-yl)-2-butyl]imidazole-4-carboxamide (25b). Replacing 3-phenylpropanol with 4-phenylbutanol and following the same procedure as in the preparation of **25a** gave **25b** (92 mg, 78.1%). IR (neat, cm^{-1}) 3700−3000, 1668, 1250; ^1H NMR ($CDCl_3$) δ −0.10 (3H, s), −0.08 (3H, s), 0.80 (9H, s), 1.75−2.00 (4H, m), 2.20−2.80 (4H, m), 3.60−4.25 (7H, m), 5.32 (1H, brs), 6.43 (1H, d, J = 3 Hz), 6.55 (1H, d, J = 2 Hz), 6.70−6.85 (2H, m), 6.95 (1H, brs), 7.15−7.35 (6H, m), 7.37 (1H, s), 7.48 (1H, d, J = 9 Hz), 7.80 (1H, s); MS (ESI, m/z) 561 (M + H)$^+$; $[\alpha]^{27}_D$ +8.2° (c 0.50, EtOH).

1-[(*R*)-1-Hydroxy-4-(6-(4-phenylbutoxy)indol-1-yl)-2-butyl]imidazole-4-carboxamide (6b). Replacing **15c** with **25b** and following the same procedure as in the preparation of **4c** and washing with IPE gave **6b** (72.7 mg, 100%) as an amorphous solid. IR (KBr, cm^{-1}) 3357, 3182, 1664, 1252; ^1H NMR (DMSO-d_6) δ 1.75−1.90 (4H, m), 2.10−2.40 (2H, m), 2.55−2.75 (2H, br), 3.60 (2H, t, J = 5 Hz), 3.80−4.20 (5H, m), 5.04 (1H, t, J = 5 Hz), 6.33 (1H, d, J = 3 Hz), 6.64 (1H, dd, J = 9 Hz, 2 Hz), 6.73 (1H, d, J = 2 Hz), 7.00−7.45 (9H, m), 7.70 (1H, s), 7.80 (1H, s); MS (ESI, m/z) 447 (M + H)$^+$; $[\alpha]^{27}_D$ +15.8° (c 0.50, MeOH); Anal. ($C_{26}H_{30}N_4O_3$·0.35H_2O) C, H, N.

1-[(*R*)-4-(6-Butoxyindol-1-yl)-1-(*tert*-butyldimethylsilyloxy)-2-butyl]imidazole-4-carboxamide (25d). To a solution of **23** (80 mg, 0.187 mmol) in DMF (5 mL) was added potassium carbonate (38.7 mg, 0.280 mmol) at room temperature. The reaction mixture was stirred for 30 min, 1-iodobutane (51.5 mg, 0.280 mmol) was added, and the resulting mixture was stirred for 24 h at 60−80 °C. The reaction mixture was poured into water (50 mL) and extracted with ethyl acetate. The organic layer was washed with brine, dried (Na_2SO_4), and evaporated in vacuo. The residue was purified by silica gel (3 g) chromatography eluting with $CHCl_3$/MeOH (50:1) to give **25d** (66.3 mg, 73.3%). IR (KBr, cm^{-1}) 3600−3000, 1666, 1255; ^1H NMR ($CDCl_3$) δ −0.10 (3H, s), −0.08 (3H, s), 0.81 (9H, s), 1.00 (3H, t, J = 7 Hz), 1.40−1.95 (4H, m), 2.20−2.60 (2H, m), 3.55−4.25 (7H, m), 5.39 (1H, brs), 6.43 (1H, d, J = 3 Hz), 6.58 (1H, d, J = 2 Hz), 6.78 (1H, d, J = 3 Hz), 6.80 (1H, dd, J = 9 Hz, 2 Hz), 6.97 (1H, brs), 7.38 (1H, s), 7.49 (1H, d, J = 9 Hz), 7.68 (1H, s); MS (ESI, m/z) 485 (M + H)$^+$; $[\alpha]^{28}_D$ +12.7° (c 0.50, EtOH).

1-[(*R*)-4-(6-Butoxyindol-1-yl)-1-hydroxy-2-butyl]imidazole-4-carboxamide (6d). Replacing **15c** with **25d** and following the same procedure as in the preparation of **4c** gave **6d** (40.8 mg, 92.6%) as a white solid; mp 176−178 °C; IR (KBr, cm^{-1}) 3317, 3236, 3163, 1676, 1238; ^1H NMR (DMSO-d_6) δ 0.95 (3H, t, J = 7 Hz), 1.35−1.85 (4H, m), 2.10−2.40 (2H, m), 3.50−4.20 (7H, m), 5.05 (1H, brs), 6.33 (1H, d, J = 3 Hz), 6.65 (1H, dd, J = 9 Hz, 2 Hz), 6.73 (1H, d, J = 2 Hz), 7.07 (1H, brs), 7.11 (1H, d, J = 3 Hz), 7.27 (1H, brs), 7.38 (1H, d, J = 9 Hz), 7.70 (1H, s), 7.80 (1H, s); MS (ESI, m/z) 371 (M + H)$^+$; $[\alpha]^{27}_D$ +21.5° (c 0.50, MeOH); Anal. ($C_{20}H_{26}N_4O_3$) C, H, N.

1-[(*R*)-1-(*tert*-Butyldimethylsilyloxy)-4-(6-hexyloxyindol-1-yl)-2-butyl]imidazole-4-carboxamide (25c). Replacing 1-iodobutane with 1-iodohexane and following the same procedure as in the preparation of **25d** gave **25c** (72.9 mg, 76.1%). IR (neat, cm^{-1}) 3700−3000, 1666, 1254; ^1H NMR

($CDCl_3$) δ −0.10 (3H, s), −0.08 (3H, s), 0.81 (9H, s), 0.92 (3H, t, J = 7 Hz), 1.20−1.95 (8H, m), 2.20−2.60 (2H, m), 3.55−4.25 (7H, m), 5.40 (1H, brs), 6.43 (1H, d, J = 3 Hz), 6.59 (1H, d, J = 2 Hz), 6.78 (1H, d, J = 3 Hz), 6.80 (1H, dd, J = 9 Hz, 2 Hz), 6.97 (1H, brs), 7.38 (1H, s), 7.49 (1H, d, J = 9 Hz), 7.68 (1H, s); MS (ESI, m/z) 513 (M + H)$^+$; $[\alpha]^{28}_D$ +10.4° (*c* 0.50, EtOH).

1-[(*R*)-4-(6-Hexyloxyindol-1-yl)-1-hydroxy-2-butyl]imidazole-4-carboxamide (6c). Replacing **15c** with **25c** and following the same procedure as in the preparation of **4c** gave **6c** (39.3 mg, 78.5%) as a white solid; mp 120−123 °C; IR (KBr, cm^{-1}) 3500−3000, 1662, 1252; ^{1}H NMR (DMSO-d_6) δ 0.89 (3H, t, J = 7 Hz), 1.15−1.55 (6H, m), 1.60−1.85 (2H, m), 2.10−2.40 (2H, m), 3.50−4.20 (7H, m), 5.04 (1H, brs), 6.33 (1H, d, J = 3 Hz), 6.64 (1H, dd, J = 9 Hz, 2 Hz), 6.74 (1H, d, J = 2 Hz), 7.06 (1H, brs), 7.11 (1H, d, J = 3 Hz), 7.26 (1H, brs), 7.38 (1H, d, J = 9 Hz), 7.70 (1H, s), 7.80 (1H, s); MS (ESI, m/z) 399 (M + H)$^+$; $[\alpha]^{28}_D$ +18.9° (*c* 0.50, EtOH); Anal. ($C_{22}H_{30}N_4O_3$) C, H, N.

1-{(*R*)-1-(*tert*-Butyldimethylsilyloxy)-4-[6-(3-(4-chlorophenyl)propoxy)indol-1-yl]-2-butyl}imidazole-4-carboxamide (25e). Replacing 3-phenylpropanol with 3-(4-chlorophenyl) propanol and following the same procedure as in the preparation of **25a** gave **25e** (90.5 mg, 83.4%). IR (neat, cm^{-1}) 3700−3000, 1668, 1254, 1093; ^{1}H NMR ($CDCl_3$) δ −0.10 (3H, s), −0.08 (3H, s), 0.81 (9H, s), 2.00−2.55 (4H, m), 2.83 (2H, t, J = 8 Hz), 3.60−4.25 (7H, m), 5.38 (1H, brs), 6.44 (1H, d, J = 3 Hz), 6.54 (1H, d, J = 2 Hz), 6.75−6.90 (2H, m), 6.96 (1H, brs), 7.10−7.35 (5H, m), 7.38 (1H, s), 7.49 (1H, d, J = 9 Hz), 7.67 (1H, s); MS (ESI, m/z) 581 (M + H)$^+$; $[\alpha]^{28}_D$ +7.7° (*c* 0.50, EtOH).

1-{(*R*)-4-[6-(3-(4-Chlorophenyl)propoxy)indol-1-yl]-1-hydroxy-2-butyl}imidazole-4-carboxamide (6e). Replacing **15c** with **25e** and following the same procedure as in the preparation of **4c** gave **6e** (61.6 mg, 93.6%) as an amorphous solid. IR (KBr, cm^{-1}) 3600−3000, 1658, 1250, 1088; ^{1}H NMR (DMSO-d_6) δ 1.90−2.40 (4H, m), 2.77 (2H, t, J = 8 Hz), 3.50−4.20 (7H, m), 5.05 (1H, brs), 6.34 (1H, d, J = 3 Hz), 6.67 (1H, dd, J = 9 Hz, 2 Hz), 6.70 (1H, d, J = 2 Hz), 7.08 (1H, brs), 7.12 (1H, d, J = 3 Hz), 7.15−7.45 (6H, m), 7.70 (1H, s), 7.80 (1H, s); MS (ESI, m/z) 467 (M + H)$^+$; $[\alpha]^{28}_D$ +16.6° (*c* 0.50, EtOH); Anal. ($C_{25}H_{27}ClN_4O_3$) C, H, N.

1-[(*R*)-1-Hydroxy-4-(5-(3-phenylpropoxy)indol-1-yl)-2-butyl]imidazole-4-carboxamide (7a). Replacing **15c** with **26a** and following the same procedure as in the preparation of **4c** gave **7a** (51.3 mg, 76.3%) as a white solid; mp 117−119 °C; IR (KBr, cm^{-1}) 3600−3000, 1658, 1238; ^{1}H NMR (DMSO-d_6) δ 1.90−2.40 (4H, m), 2.76 (2H, t, J = 8 Hz), 3.59 (2H, t, J = 5 Hz), 3.80−4.20 (5H, m), 5.03 (1H, t, J = 5 Hz), 6.32 (1H, d, J = 3 Hz), 6.77 (1H, dd, J = 9 Hz, 2 Hz), 6.95−7.40 (10H, m), 7.69 (1H, s), 7.78 (1H, s); MS (ESI, m/z) 433 (M + H)$^+$; $[\alpha]^{27}_D$ +37.0° (*c* 0.50, MeOH); Anal. ($C_{25}H_{28}N_4O_3$) C, H, N.

1-[(*R*)-4-(5-Hexyloxyindol-1-yl)-1-hydroxy-2-butyl]imidazole-4-carboxamide (7b). Replacing **15c** with **26b** and following the same procedure as in the preparation of **4c** gave **7b** (38.2 mg, 92.7%) as a white solid; mp 103−106 °C; IR (KBr, cm^{-1}) 3600−3000, 1658, 1238; ^{1}H NMR (DMSO-d_6) δ 0.88(3H, t, J = 7 Hz), 1.10−1.85 (8H, m), 2.10−2.40 (2H, m), 3.59 (2H, t, J = 5 Hz), 3.80−4.20 (5H, m), 5.04 (1H, t, J = 5 Hz), 6.32 (1H, d, J = 3 Hz), 6.74 (1H, dd, J = 9 Hz, 2 Hz), 6.90−7.40 (5H, m), 7.69 (1H, s), 7.78 (1H, s); MS (ESI, m/z) 399 (M + H)$^+$; $[\alpha]^{28}_D$ +35.9° (*c* 0.50, EtOH); Anal. ($C_{22}H_{30}N_4O_3$) C, H, N.

Ethyl 3-(5-Benzyloxy-1-methylindol-3-yl)acrylate (28). To an ice-cooled solution of 5-benzyloxy-1-methylindole-3-carboxaldehyde (13.0 g, 49.0 mmol) and triethyl phosphonoacetate (13.2 g, 58.8 mmol) in DMF (100 mL) was added NaH (60% in mineral oil, 2.74 g, 68.6 mmol). The mixture was stirred overnight at room temperature. The reaction mixture was poured into ice−water (700 mL) and stirred 30 min. The resulting precipitates were collected by filtration, washed with water, and dried in vacuo to give **28** (14.2 g, 86.3%) as a pale yellow solid. IR (KBr, cm^{-1}) 1703, 1280, 1228, 1176; ^{1}H NMR ($CDCl_3$) δ 1.36 (3H, t, J = 7 Hz), 3.78 (3H, s), 4.27 (2H, q, J = 7 Hz), 5.15 (2H, s), 6.30 (1H, d, J = 16 Hz), 7.03 (1H, dd, J = 9 Hz, 2 Hz), 7.15−7.60 (8H, m), 7.86 (1H, d, J = 16 Hz); MS (ESI, m/z) 336 (M + H)$^+$.

Ethyl 3-(5-benzyloxy-1-methylindol-3-yl)propionate (29). To a solution of **28** (11.7 g, 34.9 mmol) in EtOH·THF (300 mL, 2:1) was added 10% palladium on carbon (2.34 g), and the mixture was stirred under hydrogen (2 atm) for 1.5 h at room temperature. The mixture was filtered through Celite and washed with THF. The filtrate was concentrated in vacuo to give **29** (10.6 g, 90.0%) as a pale-yellow oil. IR (neat, cm^{-1}) 1730, 1236; ^{1}H NMR ($CDCl_3$) δ 1.25 (3H, t, J = 7 Hz), 2.66 (2H, t, J = 8 Hz), 3.04 (2H, t, J = 8 Hz), 3.71 (3H, s), 4.14 (2H, q, J = 7 Hz), 5.11 (2H, s), 6.84 (1H, s), 6.96 (1H, dd, J = 9 Hz, 2 Hz), 7.12 (1H, d, J = 2 Hz), 7.18 (2H, d, J = 9 Hz), 7.30−7.55 (5H, m); MS (ESI, m/z) 338 (M + H)$^+$.

3-(5-Benzyloxy-1-methylindol-3-yl)propionaldehyde (30). Under nitrogen, to a stirred solution of **29** (12.0 g, 35.6 mmol) in CH_2Cl_2 (120 mL) was added dropwise 1.0 M DIBAL-H in hexane (37.4 mL, 35.6 mmol) at −78 °C (dry ice/acetone) for 25 min. After 30 min, MeOH (5.7 mL) was added dropwise at −78 °C, and the mixture was stirred at room temperature for 30 min. The mixture was filtered through Celite and washed with CH_2Cl_2. The filtrate was concentrated in vacuo, and then the residue was purified by silica gel (90 g) chromatography eluted with toluene/EtOAc (10:1 to 5:1) to give **30** (8.03 g, 77.0%). IR (KBr, cm^{-1}) 1712, 1223; ^{1}H NMR ($CDCl_3$) δ 2.80 (2H, t, J = 7 Hz), 3.05 (2H, t, J = 7 Hz), 3.71 (3H, s), 5.12 (2H, s), 6.82 (1H, s), 6.97 (1H, dd, J = 9 Hz, 2 Hz), 7.09 (1H, d, J = 2 Hz), 7.15−7.55 (6H, m), 9.83 (1H, s); MS (ESI, m/z) 294 (M + H)$^+$.

5-Benzyloxy-3-(3-butenyl)-1-methylindole (31). Methyltriphenylphosphonium bromide (Ph_3PMeBr) (13.6 g, 37.9 mmol) was dried in vacuo for 2 h and then suspended with stirring in THF (150 mL) under nitrogen. The mixture was cooled to −78 °C, and 1.5 M *n*-BuLi in THF (25.3 mL, 37.9 mmol) was added dropwise. After stirring for 2 h while warming to room temperature, the mixture was again cooled to −78 °C, and **30** (7.95 g, 27.1 mmol) in THF (50 mL) was added dropwise. After 2 h at room temperature, the reaction was quenched by addition of aqueous ammonium chloride. This mixture was then extracted with EtOAc, and the extracts were washed with brine, dried ($MgSO_4$), and evaporated in vacuo. The residue was purified by silica gel (120 g) chromatography eluting with hexane/EtOAc (10:1) to give **31** (6.92 g, 87.7%) as a white solid. IR (KBr, cm^{-1}) 1223; ^{1}H NMR ($CDCl_3$) δ 2.43 (2H, q, J = 7 Hz), 2.79 (2H, t, J = 7 Hz), 3.71 (3H, s), 4.90−5.20 (4H, m), 5.80−6.05 (1H, m), 6.82 (1H, s), 6.95 (1H, dd, J = 9 Hz, 2 Hz), 7.12 (1H, d, J = 2 Hz), 7.18 (1H, d, J = 9 Hz), 7.30−7.55 (5H, m); MS (ESI, m/z) 292 (M + H)$^+$.

(*S*)-4-(5-Benzyloxy-1-methylindol-3-yl)butane-1,2-diol (32). To a mixture of *tert*-butyl alcohol (124 mL) and water (124 mL) was added AD-mix-α (34.6 g). The mixture was stirred at room temperature until both phases were clear and then cooled to 0 °C. Compound **31** (7.20 g, 24.7 mmol) was added, and the heterogeneous slurry was stirred vigorously at 0 °C for 4 h. With stirring at 0 °C, solid sodium sulfite (37.1 g) was then added and the mixture allowed to warm to room temperature and stirred for 1 h. This mixture was extracted with EtOAc, and the extracts were washed with brine, dried ($MgSO_4$), and evaporated in vacuo. The residue was purified by silica gel (215 g) chromatography eluting with $CHCl_3$/MeOH (100:1 to 20:1) to give **32** (4.30 g, 53.5%). IR (KBr, cm^{-1}) 3365, 1227, 1055; ^{1}H NMR ($CDCl_3$) δ 1.65−1.95 (3H, m), 2.03 (1H, d, J = 4 Hz), 2.70−3.00 (2H, m), 3.35−3.90 (6H, m), 5.12 (2H, s), 6.83 (1H, s), 6.96 (1H, dd, J = 9 Hz, 2 Hz), 7.11 (1H, d, J = 2 Hz), 7.18 (1H, d, J = 9 Hz), 7.30−7.55 (5H, m); MS (ESI, m/z) 326 (M + H)$^+$; $[\alpha]^{24}_D$ −21.6° (*c* 0.50, EtOH).

(*S*)-4-(5-Benzyloxy-1-methylindol-3-yl)-1-(*tert*-butyldimethylsilyloxy)butan-2-ol (33). To an ice-cooled solution of **32** (4.25 g, 13.1 mmol) in DMF (40 mL) was added imidazole (2.67 g, 39.2 mmol) followed by TBSCl (2.07 g, 13.7 mmol). After 30 min, the ice-bath was removed, and then the mixture was stirred overnight at room temperature. The reaction mixture was poured into water (100 mL) and extracted with EtOAc. The organic layer was washed with brine, dried

($MgSO_4$), and concentrated in vacuo. The residue was purified by silica gel (105 g) column chromatography eluting with hexane/EtOAc (20:1) to give **33** (4.85 g, 84.5%) as a colorless oil. IR (neat, cm^{-1}) 3458, 1252; ^1H NMR ($CDCl_3$) δ 0.07 (6H, s), 0.90 (9H, s), 1.65−1.90 (2H, m), 2.44 (1H, d, J = 4 Hz), 2.65−3.05 (2H, m), 3.30−3.85 (6H, m), 5.11 (2H, s), 6.83 (1H, s), 6.95 (1H, dd, J = 9 Hz, 2 Hz), 7.13 (1H, d, J = 2 Hz), 7.18 (1H, d, J = 9 Hz), 7.30−7.55 (5H, m); MS (ESI, m/z) 440 (M + H) $^+$; $[\alpha]^{23}_D$ −25.5° (c 0.50, EtOH).

1-[(*R*)-1-Hydroxy-4-(1-methyl-5-(3-phenylpropoxy)indol-3-yl)-2-butyl]imidazole-4-carboxamide (8a). Replacing **15c** with **36a** and following the same procedure as in the preparation of **4c** gave **8a** (26.2 mg, 99.8%) as a white solid; mp 116−119 °C; IR (KBr, cm^{-1}) 3700−3000, 1653, 1236; ^1H NMR (DMSO-d_6) δ 1.90−2.20 (4H, m), 2.30−2.60 (2H, m), 2.77 (2H, t, J = 8 Hz), 3.50−3.80 (5H, m), 3.95 (2H, t, J = 6 Hz), 4.15 (1H, m), 4.99 (1H, t, J = 5 Hz), 6.78 (1H, dd, J = 9 Hz, 2 Hz), 6.86 (1H, d, J = 2 Hz), 6.90−7.40 (9H, m), 7.73 (1H, s), 7.77 (1H, s); MS (ESI, m/z) 447 (M + H) $^+$; $[\alpha]^{27}_D$ +24.6° (c 0.50, EtOH); Anal. ($C_{26}H_{30}N_4O_3$?0.3H_2O) C, H, N.

1-[(*R*)-4-(5-Hexyloxy-1-methylindol-3-yl)-1-hydroxy-2-butyl]imidazole-4-carboxamide (8b). Replacing **15c** with **36b** and following the same procedure as in the preparation of **4c** gave **8b** (38.8 mg, 93.5%) as a white solid; mp 136−139 °C; IR (KBr, cm^{-1}) 3600−3000, 1676, 1227; ^1H NMR (DMSO-d_6) δ 0.88 (3H, t, J = 7 Hz), 1.10−1.55 (6H, m), 1.60−1.80 (2H, m), 2.00−2.20 (2H, m), 2.35−2.60 (2H, m), 3.50−3.80 (5H, m), 3.93 (2H, t, J = 6 Hz), 4.15 (1H, m), 4.99 (1H, t, J = 5 Hz), 6.75 (1H, dd, J = 9 Hz, 2 Hz), 6.86 (1H, d, J = 2 Hz), 6.90−7.35 (4H, m), 7.72 (1H, s), 7.77 (1H, s); MS (ESI, m/z) 413 (M + H) $^+$; $[\alpha]^{27}_D$ +30.3° (c 0.50, MeOH); Anal. ($C_{23}H_{32}N_4O_3$) C, H, N.

1-{(*R*)-4-[5-(3-(4-Chlorophenyl)propoxy)-1-methylindol-3-yl]-1-hydroxy-2-butyl}imidazole-4-carboxamide (8c). Replacing **15c** with **36c** and following the same procedure as in the preparation of **4c** gave **8c** (228 mg, 70.5%) as an amorphous solid. IR (KBr, cm^{-1}) 3600−3000, 1658, 1232, 1082; ^1H NMR (DMSO-d_6) δ 1.90−2.25 (4H, m), 2.30−2.60 (2H, m), 2.77 (2H, t, J = 8 Hz), 3.55−3.80 (5H, m), 3.94 (2H, t, J = 6 Hz), 4.15 (1H, m), 4.99 (1H, t, J = 5 Hz), 6.77 (1H, dd, J = 9 Hz, 2 Hz), 6.85 (1H, d, J = 2 Hz), 6.95−7.45 (8H, m), 7.72 (1H, s), 7.77 (1H, s); MS (ESI, m/z) 481 $(M + H)^+$ (^{35}Cl), 483 $(M + H)^+$ (^{37}Cl); $[\alpha]^{27}_D$ +21.3° (c 0.50, EtOH); Anal. ($C_{26}H_{29}ClN_4O_3$·0.3H_2O) C, H, N.

Biological Methods. Expression and purification of human recombinant ADA as well as in vitro ADA enzyme assay have been described previously.[19]

Crystallography of 4e/ADA. Cocrystals of the bovine intestine ADA were obtained using procedures similar to those previously described.[27] In this study, 100 mM MES, pH 6.0, 2.1 M ammonium sulfate, and 2.5% (v/v) PEG-400 were used as precipitant. X-ray diffraction data were collected from this $P4_32_12$ form: a = 78.37 Å, c = 137.82 Å, at SP-ring8 beamline 24XU. Data resolution was from 51.75 to 2.25 Å; 137589 observations were scaled and merged into 20752 unique reflections using Crystal Clear (RIGAKU). The overall R-merge was 9.0%, the ratio $I/\sigma(I)$ was 8.7, and the data 98.1% complete. Corresponding values for the high-resolution data shell (2.35−2.25 Å) are 33.8%, 3.0, and 96.6%, respectively. The structure of the **4e**/ADA complex was solved and refined using these data, program AMoRe[28] and X-PLOR (Accelrys), and the protein model 1KRM from the Protein Data Bank.[29] The conventional and free R-factors after refinement are 23.2% and 25.3%. The rms deviations between model and ideal bond distances, bond angles, dihedral angles, and improper angles are 0.021 Å, 3.9°, 26.7°, and 2.98°. The model coordinates have been deposited in the Protein Data Bank with the code 1QXL.

Crystallography of 4c/ADA. Cocrystals of the bovine intestine ADA were obtained using procedures similar to the **4e**/ADA complex. X-ray diffraction data were collected from this $P4_32_12$ form: a = 78.32 Å, c = 138.32 Å, at SP-ring8 beamline 24XU. Data resolution was from 37.68 to 2.5 Å; 89568 observations were scaled and merged into 15505 unique reflections using Crystal Clear (RIGAKU). The overall R-merge was 10.3%, the ratio $I/\sigma(I)$ was 4.5, and the data 99.7% complete. Corresponding values for the high-resolution data shell (2.66−2.50 Å) are 28.9%, 2.6, and 98.5%, respectively. The structure of the **4c**/ADA complex was solved and refined using these data, program AMoRe[28] and X-PLOR (Accelrys), and the protein model from the **4e**/ADA complex. The conventional and free R-factors after refinement are 22.6% and 28.6%. The rms deviations between model and ideal bond distances, bond angles, dihedral angles, and improper angles are 0.036 Å, 5.3°, 27.8°, and 3.98°. The model coordinates have been deposited in the Protein Data Bank with the code 1UML.

Crystallography of 5/ADA. Cocrystals of the bovine intestine ADA were obtained using procedures similar to the **4e**/ADA complex. X-ray diffraction data were collected from this $P4_32_12$ form: a = 78.44 Å, c = 137.71 Å, at SP-ring8 beamline 24XU. Data resolution was from 51.75 to 2.35 Å; 238710 observations were scaled and merged into 19201 unique reflections using Crystal Clear (RIGAKU). The overall R-merge was 7.4%, the ratio $I/\sigma(I)$ was 2.0, and the data 98.9% complete. Corresponding values for the high-resolution data shell (2.50−2.35 Å) are 35.2%, 6.3, and 99.4%, respectively. The structure of the **5**/ADA complex was solved and refined using these data, program AMoRe[28] and X-PLOR (Accelrys), and the protein model from the **4e**/ADA complex. The conventional and free R-factors after refinement are 22.8% and 24.2%. The rms deviations between model and ideal bond distances, bond angles, dihedral angles, and improper angles are 0.042 Å, 5.0°, 26.7°, and 4.90°. The model coordinates have been deposited in the Protein Data Bank with the code 1O5R.

Docking Simulation. Inhibitor molecules were modeled based on the active conformation of **1**, taken from the crystal structure of **1**/ADA complex, using InsightII(Accelrys). The modeled structures were energy minimized by Discover-(Accelrys) adopting the cvff force field parameters. The initial binding status of each inhibitor molecule was simulated using GREEN(IMMD) in the following way: the modeled compound was placed at the active site manually referring to the crystal structure of **1**/ADA complex, and energetically stable conformations were explored using the Monte Carlo simulation mode considering the flexibility of the rotatable bonds. The binding mode which gave the most stable interaction energy was adopted as initial binding status. This binding status was further minimized by Discover(Accelrys) using the following protocol: main chain atoms of ADA were set fixed to the original position during the minimization, positions of side chain atoms of the residues coordinating to the zinc atom, that is His15, His17, His214 and Asp295, were also fixed. In addition, one water molecule that coordinates to Zn and two water molecules that form hydrogen bonds with the carboxamide moiety of **1**, were fixed. Other non-hydrogen atoms were tethered at the original position with a force constant of 25 kcal/Å. The minimization of the whole complex structure was carried out by 50 steps of the steepest descent method followed by 10000 steps of the conjugate gradient method until the maximum derivative is less than 0.1 kcal/Å. The interaction energies between ADA and inhibitor molecules are obtained by InsightII(Accelrys) based on the minimized complex structures.

Rat Pharmacokinetic Study. Male Sprague−Dawley rats, weighing between 300 and 350 g, were used. The animals were housed in a controlled room at 20−26 °C with a 12 h light/dark cycle. Food and water were provided ad libitum. After overnight fasting, rats were used for pharmacokinetic experiments. For intravenous dosing, compound **8c** solution was injected into the femoral vein at a dose of 10 mg/kg to rats. For oral dosing, the solution was given by gavage at a dose of 10 mg/kg to rats. Blood samples were collected at 0.083, 0.25, 0.5, 1, 2, 4, 6, and 8 h after intravenous administration and 0.25, 0.5, 1, 2, 4, 6, and 8 h after oral administration. Blood samples were collected in heparinized tubes and then centrifuged to separate plasma samples. All samples were stored on ice until analyzed. Plasma samples were added into methanol to precipitate protein and centrifuged. Aliquots of the supernatant were injected into HPLC for assay.

Acknowledgment. We thank Dr. David Barrett, Fujisawa Pharmaceutical Co. Ltd., for valuable comments and help in the preparation of the manuscript.

Supporting Information Available: Description of the synthesis and experimental data for the preparation of compounds **17**−**22**, **24**, **26**, and **34**−**36**. This material is available free of charge via the Internet at http://pubs.acs.org.

References

(1) Cronstein. B. N. Adenosine, An endogenous antiinflammatory agent. *J. Appl. Physiol.* **1994**, *76*, 5−13.
(2) Ohta, A.; Sitkovsky, M. Role of G-protein-coupled adenosine receptors in downregulation of inflammation and protection from tissue damage. *Nature* **2001**, *414*, 916−920.
(3) (a) Rudolphi, K. A.; Schubert, P.; Parkinson, F. E.; Fredholm, B. B. Neuroprotective role of adenosine in cerebral ischemia. *Trends. Pharmacol. Sci.* **1992**, *13*, 439−445. (b) Marquardt, D. L.; Gruber, H. E.; Wasserman, S. I. Adenosine release from stimulated mast-cells. *Proc. Natl. Acad. Sci. U.S.A.* **1984**, *81*, 6192−6196. (c) Filippini, A.; Taffs, R. E.; Sitkovsky, M. V. Extracellular ATP in T-lymphocyte activation: Possible role in effector functions. *Proc. Natl. Acad. Sci. U.S.A.* **1990**, *87*, 8267−8271.
(4) (a) Cronstein, B. N.; Naime, D.; Ostad, E. The antiinflammatory mechanism of Methotrexate. Increased adenosine release at inflamed sites diminishes leukocyte accumulation in an in vivo model of inflammation. *J. Clin. Invest.* **1993**, *92*, 2675−2682. (b) Cronstein, B. N.; Montesinos, M. C.; Weissmann, G. Sites of action for future therapy: an adenosine-dependent mechanism by which aspirin retains its antiinflammatory activity in cyclooxygenase-2 and NFκB knockout mice. *Osteoarthritis Cartilage* **1999**, *7*, 361−363. (c) Cronstein, B. N.; Montesinos, M. C.; Weissmann, G. Salycylates and sulfasalazine but not glucocorticoids, inhibit leukocyte accumulation by an adenosine-dependent mechanism that is independent of inhibition of prostaglandin synthesis and p105 of NFkB. *Proc. Natl. Acad. Sci. U.S.A.* **1999**, *96*, 6377−6381.
(5) Cristalli, G.; Costanzi, S.; Lambertucci, C.; Lupidi, G.; Vittori, S.; Volpini, R.; Camaioni, E. Adenosine deaminase: Functional implications and different classes of inhibitors. *Med. Res. Rev.* **2001**, *21*, 105−128.
(6) Resta, R.; Thompson, L. F. SCID: the role of adenosine deaminase deficiency. *Immunol. Today* **1997**, *18*, 371−374.
(7) Kameoka, J.; Tanaka, T.; Nojima, Y.; Schlossman, S. F.; Morimoto, C. Direct association of adenosine deaminase with T cell activation antigen, CD26. *Science* **1993**, *261*, 466−469.
(8) (a) Franco, R.; Valenzuela, A.; Lluis, C.; Blanco, J. Enzymatic and extraenzymatic role of ecto-adenosine deaminase in lymphocytes. *Immunol. Rev.* **1998**, *161*, 27−42. (b) Morimoto, C.; Schlossman, S. F. The structure and function of CD26 in the T-cell immune response. *Immunol. Rev.* **1998**, *161*, 55−70.
(9) Agerwal, R. P.; Spector, T.; Parks, R. E. Tight-binding inhibitors IV. Inhibition of adenosine deaminase by various inhibitors. *Biochem. Pharmacol.* **1977**, *26*, 359−367.
(10) Rafel, M.; Cervantes, F.; Beltran, J. M.; Zuazu, J.; Nieto, L. H.; Rayon, C.; Talavera, J. G.; Montserrat, E. Deoxycoformycin in the treatment of patients with hairy cell leukemia. *Cancer* **2000**, *88*, 352−357.
(11) Brogden, R. N.; Sorkin, E. M. Pentostatin. A review of its pharmacodynamic and pharmacokinetic properties, and therapeutic potential in lymphoproliferative disorders. *Drugs* **1993**, *46*, 652−677.
(12) McConnell, W. R.; Furner, R. L.; Hill, D. L. Pharmacokinetics of 2′-deoxycoformycin in normal and L1210 leukemic mice. *Drug Metab. Dispos.* **1979**, *7*, 11−13.
(13) Lathia, C.; Fleming, G. F.; Meyer, M.; Ratain, M. J.; Whitfield, L. Pentostatin pharmacokinetics and dosing recommendations in patients with mild renal impairment. *Cancer Chemother. Pharmacol.* **2002**, *50*, 121−126.
(14) (a) Baker, D. C.; Hanvey, J. C.; Hawkins, L. D.; Murphy, J. Identification of the bioactive enantiomer of *erythro*-3-(adenine-9-yl)-2-nonanol (EHNA), a semi-tight binding inhibitor of adenosine deaminase. *Biochem. Pharmacol.* **1981**, *30*, 1159−1160. (b) Bessodes, M.; Bastian, G.; Abushanab, E.; Panzica, R. P.; Berman, S. F.; Marcaccio, E. J.; Chen, S. F.; Stoeckler, J. D.; Parks, R. J. Effect of chirality in *erythro*-9-(2-hydroxy-3-nonyl) adenine (EHNA) on adenosine deaminase inhibition. *Biochem. Pharmacol.* **1982**, *31*, 879−882.
(15) Cristalli, G.; Eleuteri, A.; Franchetti, P.; Grifantini, M.; Vittori. S.; Lupidi, G. Adenosine deaminase inhibitors: Synthesis and structure−activity relationships of imidazole analogue of *erythro*-9-(2-hydroxy-3-nonyl) adenine. *J. Med. Chem.* **1991**, *34*, 1187−1192.
(16) Pragnacharyulu, P. V. P.; Varkhedkar, V.; Curtis, M. A.; Chang, I. F.; Abushanab, E. Adenosine deaminase inhibitors: Synthesis and biological evaluation of unsaturated, aromatic, and oxo derivatives of (+)-*erythro*-9-(2′*S*-hydroxy-3′*R*-nonyl) adenine [(+)-EHNA]. *J. Med. Chem.* **2000**, *43*, 4694−4700.
(17) McConnell, W. R.; El-Dareer, S. M.; Hill, D. L. Metabolism and disposition of *erythro*-9-(2-hydroxy-3-nonyl)[^{14}C] adenine in the rhesus monkey. *Drug Metab. Dispos.* **1980**, *8*, 5−7.
(18) Lambe, C. U.; Nelson, D. J. Pharmacokinetics of inhibition of adenosine deaminase by *erythro*-9-(2-hydroxy-3-nonyl) adenine in CBA mice. *Biochem. Pharmacol.* **1982**, *31*, 535−539.
(19) Terasaka, T.; Nakanishi, I.; Nakamura, K.; Eikyu, Y.; Kinoshita, T.; Nishio, N.; Sato, A.; Kuno, M.; Seki, N.; Sakane, K. Structure-based de novo design of non-nucleoside adenosine deaminase inhibitors. *Bioorg. Med. Chem. Lett.* **2003**, *13*, 1115−1118.
(20) Terasaka, T.; Kinoshita,T.; Kuno, M.; Nakanishi, I. A highly potent non-nucleoside adenosine deaminase inhibitor: Efficient drug discovery by intentional lead hybridization. *J. Am. Chem. Soc.* **2004**, *126*, 34−35.
(21) Agerwal, R. P. Inhibitors of adenosine deaminase. *Pharmacol. Ther.* **1982**, *17*, 399−429.
(22) Alberg, D. G.; Schreiber, S. L. Structure-based design of a cyclophilin-calcineurin bridging ligand. *Science* **1993**, *262*, 248−250.
(23) Lipinski, C. A.; Lombardo, F.; Dominy, B. W.; Feeney, P. J. Experimental and computational approaches to estimate solubility and permeability in drug discovery and development settings. *Adv. Drug Delivery Rev.* **1997**, *23*, 3−25.
(24) Smith, D. A.; Jones, B. C.; Walker, D. K. Design of drugs involving the concepts and theories of drug metabolism and pharmacokinetics. *Med. Res. Rev.* **1996**, *16*, 243−266.
(25) Terasaka, T.; Seki, N.; Tsuji, K.; Nakanishi, I.; Kinoshita,T.; Nakamura, K. WO 00/55155, 2000.
(26) Sharpless, K. B.; Amberg, W.; Bennani, Y. L.; Crispino, G. A.; Hartung, J.; Jeong, K. S.; Kwong, H. L.; Morikawa, K.; Wang, Z. M.; Xu, D. Q.; Zhang, X. L. The osmium-catalyzed asymmetric dihydroxylation: A new ligand class and a process improvement. *J. Org. Chem.* **1992**, *57*, 2768−2771.
(27) Kinoshita, T.; Nishio, N.; Sato, A.; Murata, M. Crystallization and preliminary analysis of bovine adenosine deaminase. *Acta Crystallogr.* **1999**, *D55*, 2031−2032.
(28) Navaza, J. On the computation of the fast rotation function. *Acta Crystallogr.* **1993**, *D49*, 588−591.
(29) Kinoshita, T.; Nishio, N.; Nakanishi, I.; Sato, A.; Fujii, T. Crystal structure of bovine adenosine deaminase complexed with 6-hydroxyl-1,6-dihydropurine riboside. *Acta Crystallogr.* **2003**, *D59*, 299−303.

JM0306374